Article

A Cyber-Physical Prototyping and Testing Framework to Enable the Rapid Development of UAVs

Or D. Dantsker * ⓘ, Mirco Theile ⓘ and Marco Caccamo ⓘ

Chair of Cyber-Physical Systems in Production Engineering, TUM School of Engineering and Design, Technical University of Munich, Boltzmannstr. 15, D-85748 Garching, Germany; mirco.theile@tum.de (M.T.); mcaccamo@tum.de (M.C.)
* Correspondence: or.dantsker@tum.de

Abstract: In this work, a cyber-physical prototyping and testing framework to enable the rapid development of UAVs is conceived and demonstrated. The UAV Development Framework is an extension of the typical iterative engineering design and development process, specifically applied to the rapid development of UAVs. Unlike other development frameworks in the literature, the presented framework allows for iteration throughout the entire development process from design to construction, using a mixture of simulated and real-life testing as well as cross-aircraft development. The framework presented includes low- and high-order methods and tools that can be applied to a broad range of fixed-wing UAVs and can either be combined and executed simultaneously or be executed sequentially. As part of this work, seven novel and enhanced methods and tools were developed that apply to fixed-wing UAVs in the areas of: flight testing, measurement, modeling and emulation, and optimization. A demonstration of the framework to quickly develop an unmanned aircraft for agricultural field surveillance is presented.

Keywords: UAVs; design; cyber-physical; prototyping; simulation; flight testing

1. Introduction

In recent years, we have seen an uptrend in the popularity of unmanned aerial vehicles (UAVs) driven by the desire to apply these aircraft to a variety of civilian, commercial, education, and government applications. These applications include precision farming, infrastructure inspection, environment monitoring, surveillance, surveying and mapping, search and rescue missions, rapid assessment of emergency situations and natural disasters, next generation Internet connectivity, and weather forecasting, among many others. In the United States alone, there are over a million individuals that are registered to operate these aircraft [1].

Accompanying the uptrend in UAV use over the past several years, there has been an increase in research to evaluate and improve aircraft performance and flight characteristics. For example, significant effort has been put into studying aerodynamic qualities [2,3], especially in high angle-of-attack conditions [4–6], as well as in the development of new control algorithms [7–10]. There have also been studies of UAV performance through stall or upset maneuvers [11–14]. In addition, new aircraft configurations [15–18] and flight control hardware and software [19–23] have been tested. Research evaluating aircraft power consumption reduction through steady and dynamic soaring has also become the subject of significant attention recently [24–28]. However, there has been little attention towards improving the design and development process of UAVs that could be quickly prototyped.

Most aircraft design and development processes typically start with a requirement phase followed by conceptual design. The conceptual design phase is made up of many individual steps, including platform layout, component sizing, mass estimation, and analysis for desired mission performance. The many individual steps iterate in series and

in parallel until an optimum solution is found. A feasibility study also often occurs as part of conceptual design. This process is often portrayed as a tree with a web of interconnected steps [29–36] or as a design wheel [37–39]. Once the conceptual design is finalized, the overall configuration is frozen and the design process moves on to preliminary design, generally without further major iteration.

During preliminary design, specific design elements are analyzed and evaluated in more detail, yielding a more refined and matured design. This is followed by detailed design and development, where a producible design is created. During the detailed design process, a go-ahead is given to begin manufacturing and testing. Once a prototype is developed, flight testing and evaluation begin with effort made toward aircraft certification. Full-scale production of the aircraft occurs in the late stages of certification or after it is complete. Only in cases where requirements are not met, e.g., failing to meet performance benchmarks or not passing certification, does the development process revert significantly with the rework of the aircraft design [40,41]. These design rework iterations are very costly and should be avoided whenever possible.

In order to enhance the aircraft design and development process, multi-discipline analysis (MDA) and optimization (MDO) are increasingly integrated into the conceptual or preliminary design stages [42–47]. MDO allows for significant inter-weaved and interdisciplinary process iterations within the various design stages, i.e., enabling set-based design iteration processes [48]. Yet these set-based design iterations are generally constrained before fabrication or manufacturing occur due to the high cost involved in aircraft modification. Recent efforts have looked into integrating the use of MDO into the entire design process of UAVs, including optimized and automated detail design [49,50].

To truly enable an agile UAV development process, this work conceives and demonstrates a cyber-physical prototyping and testing framework to enable the rapid development of UAVs, called the UAV Development Framework. The development framework is an extension of the typical iterative engineering design and development process, specifically applied to the development of UAVs. However, unlike other development frameworks in the literature, the framework allows for straightforward rework iteration throughout the entire development process from design to construction, using a mixture of simulated and real-life testing as well as cross-aircraft development. The framework (in the form presented) includes a variety of low- and high-order methods and tools that can be applied to a broad range of fixed-wing UAVs and can either be combined and run simultaneously or be run sequentially. For specific aircraft or application requirements, methods and tools can be added, removed, or modified as need be within the framework. As part of this work, seven novel and enhanced methods and tools that apply to fixed-wing UAVs were developed; these include methods and tools in the areas of: flight testing, measurement, modeling and emulation, and optimization.

This work is structured as follows: Section 2 describes the UAV Development Framework, including its structure and functionality. Then, in Section 3, the novel and enhanced methods and tools used in the framework are described in greater detail. Section 4 then presents an example demonstration of the framework: to quickly develop an unmanned aircraft for agricultural field surveillance. The paper concludes in Section 5.

2. Framework

The UAV Development Framework was developed to enable the rapid prototyping and testing of unmanned aircraft through the iterative use of methods and tools. In order to minimize development time, the framework enables cross-aircraft development where aircraft systems, or even methods or tools, can be developed on a different (existing) aircraft and then be applied to the aircraft of interest. A functional diagram of the framework is shown in Figure 1.
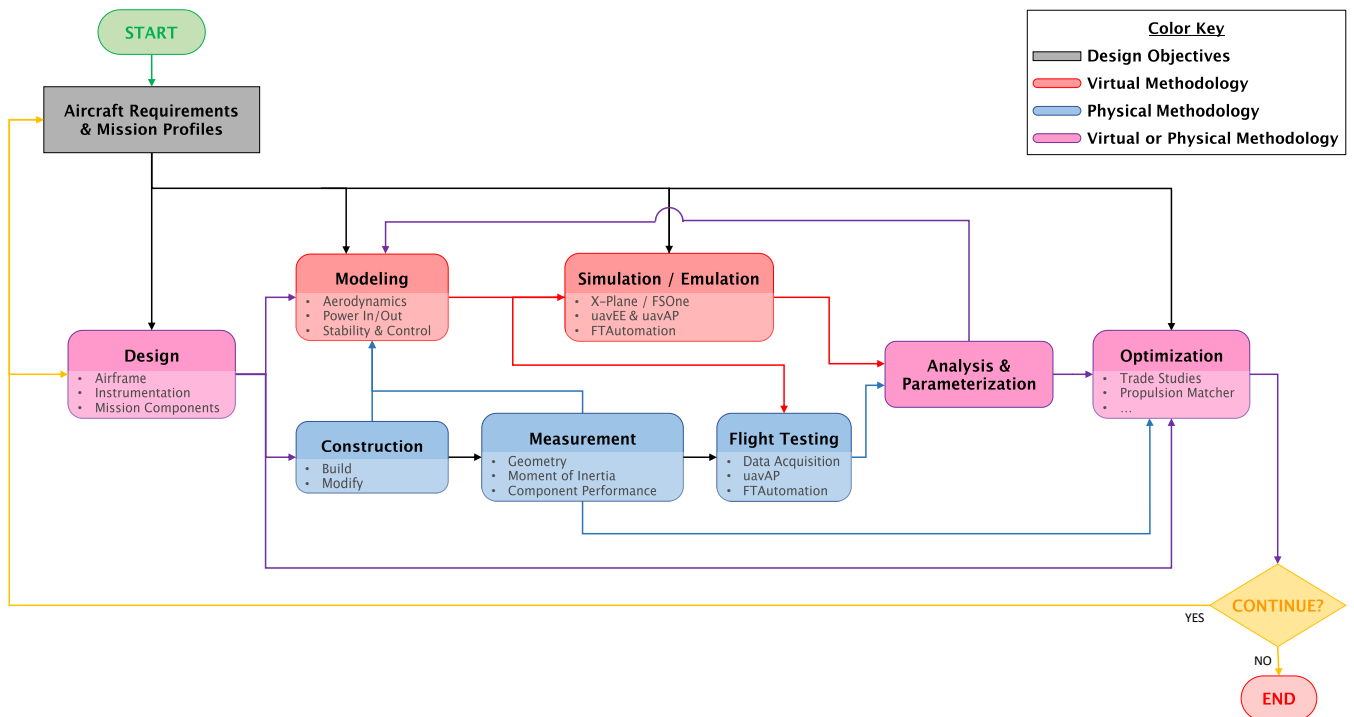
Figure 1. A functional diagram of the UAV Development Framework.

In the development framework, once arriving at a given step, one can choose to advance to any or all subsequent steps that are connected by an arrow; this allows one to drop into either design or straight into modeling or simulation and then iterate within that cycle. Additionally, each step is shown with a small list of methods and tools below—these methods and tools were chosen or developed to be sufficiently generalized for the majority of electric-powered, propeller-driven, fixed-wing unmanned aircraft. However, they could be substituted as needed for other aircraft; thus, the lists of methods and tools are not supposed to be comprehensive lists but rather an example based on what was developed in this work. Below, a detailed description is given of the flow and iterations possible within the framework. An overview of the methods and tools mentioned is provided in Section 3.

Framework Flow and Iteration

As can be seen in the diagram, the UAV development effort begins at the top left with *Aircraft Requirements & Mission Profiles*. Once these are defined, *Design*, *Modeling*, *Simulation/Emulation*, or *Optimization* can occur. As mentioned above, it is possible and expected that *Design* and *Optimization* occur repeatedly until the user determines that the aircraft design is ready to proceed to initial testing, either virtually (boxes in red) or physically (boxes in blue). The *Design* operation considers the airframe, instrumentation, and mission components of an aircraft, among others. The *Optimization* operation can include contemporary methods such as Trade Studies or the recently developed *Propulsion System Optimization Tool* [51] (Propulsion Matcher in the diagram).

It is also possible that the user chooses to start through *Simulation/Emulation* using existing aircraft designs, performs *Analysis & Parameterization*, and then proceeds to *Optimization* and, if need be, iterates within that design loop. The design loop can also be executed through a full virtual cycle, passing through *Design, Modeling, Simulation/Emulation, Analysis & Parameterization*, and *Optimization*, again, potentially reworking an existing design. *Modeling* considers aerodynamics, power balance, and stability and control, among other factors; for example, with the *Electric Aircraft Power Consumption Model* [52]. *Simulation/Emulation* is based on the *uavEE* emulation environment using X-Plane 11 [53] or FS One [54] for simulation; one may also use the *uavAP* autopilot's *Flight Testing Automation* tool [55] to aid

in acquiring easily parameterizable flight data. Proceeding through any of these virtual design loops offers the user quick rework iteration at minimal cost.

Once the user decides they are ready to proceed from design to a physical development option, some type of *Construction* will occur of the aircraft, a sub-scale model, or of sub-components. Subsequent passes through *Construction* will either yield *Modification* to the existing physical platform(s) or complete *Build(s)*. Once physical development occurs, the next step is to perform *Measurement(s)* of what has been constructed. If, say, only the propulsion system has been developed, one can test its performance [56]. Alternately, if an entire aircraft has been built/modified, one may wish to measure its *Moment of Inertia* [57]. The data generated by these *Measurement(s)* can feed into *Modeling* of the vehicle or the *Optimization* methods. After *Measurement* has concluded, the subsequent step is to *Flight Test* the vehicle or sub-component. A *Data Acquisition* system [58,59] is likely to be used in *Flight Testing*. Similarly to *Simulation/Emulation*, *Flight Testing* can be performed autonomously using *Flight Testing Automation*.

Iteration of the entire design loop occurs after each pass through the *Optimization* step. If more iterations are needed, the user will *Continue* back to *Aircraft Requirements & Mission Profiles* and/or *Design*. It is expected that certain *Optimizations* may produce results that shift the entire design problem, i.e., modifying the *Aircraft Requirements & Mission Profiles*. However, once the user is satisfied with the final design, i.e., there is little reason for further work after the last *Optimization* operation, one can choose to stop iterating. This is illustrated at the bottom right of the diagram.

3. Novel and Enhanced Framework Methods and Tools

In order to design and demonstrate the proposed UAV Development Framework, several methods and tools were developed or improved and used in conjunction with contemporary methods. In the following sub-sections, these developed methods and tools are described within the scope of (1) flight testing, (2) measurement, (3) modeling and emulation, and (4) optimization. Each of these sub-sections correlates to one or more of the blocks of the UAV Development Framework, per the functional diagram presented in Figure 1.

All of the methods and tools mentioned were developed using the Avistar UAV testbed, which is shown in Figure 2. The fixed-wing aircraft has a wingspan of 1.59 m (62.5 in) and a mass of 3.7 kg (8.16 lb). Further testbed details regarding construction, physical, or component specifications can be found in related literature [60].

Figure 2. The flight-ready Avistar UAV testbed aircraft.
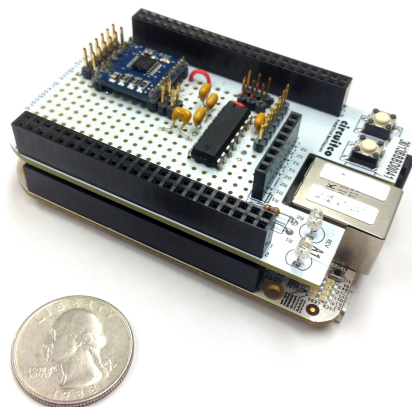
3.1. Flight Testing

Capturing accurate flight testing data is a fundamental component of the UAV Development Framework and doing so requires the acquisition of high-fidelity flight data from a large range of sensors and devices. This naturally leads one to either attain and utilize an existing data acquisition platform or to develop one's own if unable to find a system that can satisfy the requirements. In the scope of the framework, it was necessary to develop a data acquisition system as no other system that was available could satisfy the requirements

for the aircraft used in either application (presented in Section 4). Additionally, in order to support the capturing of accurate, i.e., repeatable, aircraft performance and dynamics data, a flight testing automation process was developed and integrated into a later version of the flight control and data acquisition system developed and used for this work.
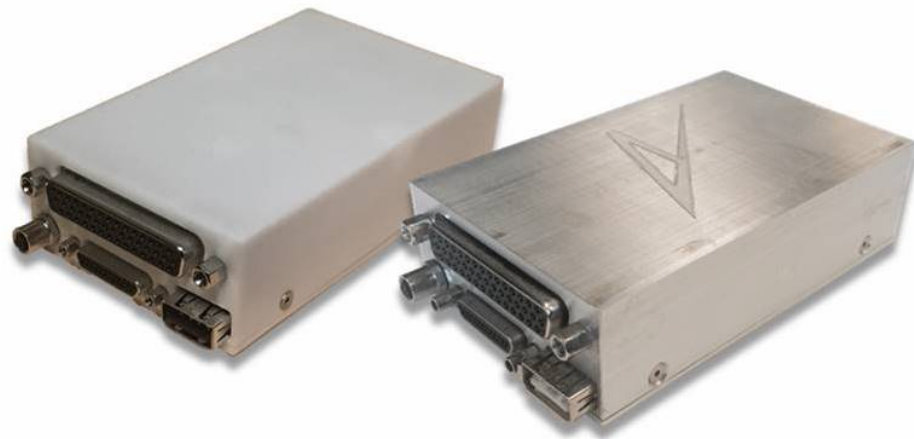
3.1.1. Data Acquisition

A high-frequency sensor data acquisition system (SDAC) was developed for flight control and aerodynamic data collection research, specifically aimed toward small to mid-sized UAVs [58,59]. The SDAC could combine many sensor streams into a unified high-fidelity state data stream and could passively record and/or simultaneously forward that data stream to a separate process, such as an autopilot, which was added on in a later commercial revision. The data acquisition system was completely fabricated out of commercial off-the-shelf (COTS) components, which reduced both cost and implementation time. The system was small, low-weight, and low-power, and operated at 100 Hz. It featured a large variety of sensors, including a 9 degree-of-freedom inertial measurement unit (IMU) with a global position system (GPS) or receiver, 3-axis magnetometer, pitot probe, electronic tachometer, seven 10-bit analog-to-digital converters (ADCs), thirty-two 12-bit analog-to-digital converters, a 14-bit analog-to-digital converter, twenty digital input/outputs (I/Os), twelve pulse width modulation (PWM) signal inputs, a 40-mile downlink transceiver, open serial, open CANbus port, and up to 64 GB of onboard storage. The handful of ADCs, I/Os, and ports allowed further expandability.

Given the included sensor and input capabilities, the system was able to simultaneously log, output, and transmit: 3D linear and angular accelerations, velocities, and position along with GPS location; pitot probe airspeed; 3D magnetic field strength and heading; control surface inputs; and control surface deflections. All of these measurements are vital for flight testing data collection. A photo of the SDAC central unit is shown in Figure 3. Over time, the SDAC platform was upgraded to provide additional capabilities. As previously mentioned, the platform was eventually used as a sensor fusion platform, providing a uniform stream of sensor data for a quad-core ARM-based flight control board. At the time of its development, the SDAC provided the greatest sensor capability at the highest acquisition rate among research-grade data acquisition systems intended for UAVs. The Al Volo FDAQ and FC+DAQ commercialized data acquisition and flight control systems, [61] shown in Figure 4, draw their lineage to the SDAC platform and have been used on over a dozen aircraft to date, including the application aircraft in this work. A comparison of the SDAC and the Al Volo commercial platforms to other comparable research institutions and commercial systems was performed in related literature [62] and showed superior capabilities and performance.

Figure 3. The developed high-frequency sensor data acquisition system SDAC.

Figure 4. The commercialized Al Volo FDAQ and FC+DAQ data acquisition and flight control systems.

3.1.2. Flight Testing Automation

Flight testing is an important milestone in the aircraft development process and is typically performed by manually piloting both full-scale aircraft and sub-scale UAVs [39]. Traditionally, flight testing maneuvers, which follow standards and generally accepted practices, are assembled into test cards and relayed by a test director to the pilot; this was the flight testing procedure for both full-scale aircraft, such as the Lockheed Martin F-35 [63] 5th generation fighter jet, and sub-scale UAVs, such as the University of Illinois GA-USTAR [64] dynamically scaled general-aviation testbed. There exist standards and generally accepted practices for flight testing maneuvers that are described and outlined in flight testing books, such as those by Kimberlin [65], McCormick [66], and Ward [67]. Due to the high cost and risks involved, significant effort has been allocated to improving the flight testing process, with researchers looking at enhanced data collection techniques. Specifically, researchers have developed aircraft flight testing parameterization methods that use human-triggered control surface excitation [68], uncorrelated/random (stick-shaker) human control inputs [69], human-control augmented with multi-sine inputs [70], and fully automated frequency sweeps [71]. However, most flight testing involving UAVs faces the additional challenge of piloting the aircraft externally in 3rd person while maintaining visual line-of-sight (VLOS) per regulatory requirements, e.g., the U.S. Federal Aviation Administration 14 CFR Part 107 [72]. Operation of UAVs outside of these requirements involves attaining special certification and/or licensing, which is outside the reach of most UAVs' flight testing efforts. Therefore, flight testing of UAVs is generally constrained to VLOS, which is generally around 500 m [73,74] but for larger, brightly painted aircraft, it can be up to 1000 m [75].

Thus, recent literature on UAVs has looked into techniques to enhance flight test pattern design and share control between a VLOS pilot and a ground station pilot. For example, Stahl et al. analyzed various flight test pattern designs, including a circle, standard race track, figure-8 race track, and 2-pilot "horse track" in order to test an active flutter suppression system on their purpose-built FLEXOP aircraft [75]. Sobron et al. used variations of race tracks, standard and figure-8, to flight test their Generic Future Fighter sub-scale demonstrator; yet, to maximize their VLOS airspace, they automated open-loop maneuvers within race tracks using a radio control transmitter that output predefined control sequences of throttle and control surface commands [74]. These predefined sequences allowed more efficient and effective evaluation of aircraft trim, loading, and control surface response; however, as the sequences were pre-programmed, i.e., open-loop, they could not respond to sensor data and thus heavily relied on accurate human-pilot setup to place the aircraft in a proper initial state. Similar techniques were previously described by Arifianto [76] and Sanders [77]. Another option to best utilize VLOS airspace was used in early testing of the NASA AirSTAR program, where a safety pilot always maintained VLOS

while a research pilot performed flight testing maneuvers from a synthetic vision and downlinked video ground station cockpit [78]. This approach was used by other flight testing campaigns that were limited to VLOS operation [79,80].

Therefore, as part of the UAV Development Framework, a flight testing automation process was developed to streamline the flight testing and parameterization process for fixed-wing unmanned aircraft constrained to operating in VLOS airspace. Flight testing automation provides substantially extended capabilities compared to previous VLOS flight testing techniques. *uavFT* is integrated into the modular, open-source *uavAP* autopilot and *uavGS* ground station interface [23]. Integrated maneuvers include: trimmed flight, turning flight, climb and descent, stall, idle descent, phugoid, singlets, doublets, and multi-sine sequences; these enable characterization of aircraft aerodynamics, longitudinal and lateral stability, and control effectiveness. The process allows the user to easily design, position, and command the aircraft through parameterizable flight testing maneuvers within the airspace. Automating the data collection process, as opposed to the previous status quo, allows for improved airspace utilization and more efficient flight testing through precise maneuvering, minimal trial-and-error, and, more importantly, decreased flight time requirements.

Flight testing automation was implemented and demonstrated using software-in-the-loop simulation in the uavEE emulation environment (described in Section 3.3.1). A comparison between automated and trained manually piloted flight was performed for testing stall using a Cessna 172 under ideal conditions in the X-Plane 11 Flight Simulator [55]. This Cessna 172 flight model was used as it is a default aircraft model in the simulator, which allows for reproducibility by any user in the community. The manually operated stall maneuver showed signs of variations and oscillations in accelerations, rotation rates, Euler angles, and angle-of-attack, pointing to difficulty exhibited by the trained human pilot in simultaneously controlling the aircraft altitude, roll, and heading. In comparison, the time history of autonomously controlled stall speed maneuver shows smooth and accurate results.

Flight testing automation was then demonstrated in experimental flight testing using the Avistar UAV. Only a subset of the maneuvers developed were demonstrated due to limited weather opportunities; these include stall speed, stall polar, idle descent, singlets, and doublet. Among the maneuvers performed during the flight tests demonstrations, a 500 ms, 50% amplitude left–right aileron doublet was repeated several times on several different days with somewhat different environmental conditions. Figure 5 shows (a) the automated control input and (b) resulting rotation rates for the first of these maneuvers performed. Likewise, Figure 5c,d show the resulting rotation rates for the second and third maneuvers performed with similar steady-state setup and identical control; note that the second and third maneuvers were performed at slightly different start times, yielding the time offset. As can be seen in the figures, the measured aircraft response for the same input is repeatedly highly similar, even though there were somewhat different environmental conditions; the response width, amplitude, and trend are consistent between maneuvers. This result therefore demonstrates the true power of using the flight test automation process, repeatability. Further details regarding the implementation, capabilities, and evaluation of the flight testing automation process can be found in related literature [55].
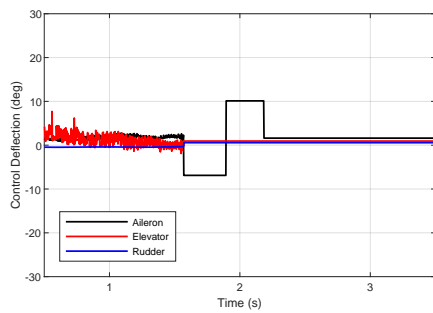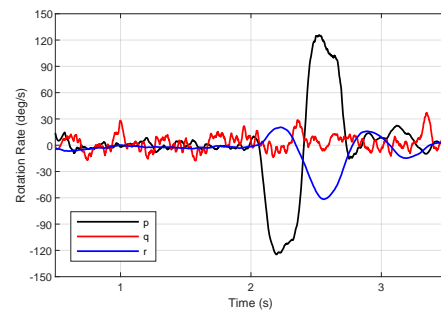
(**a**) Control input for doublet #1.
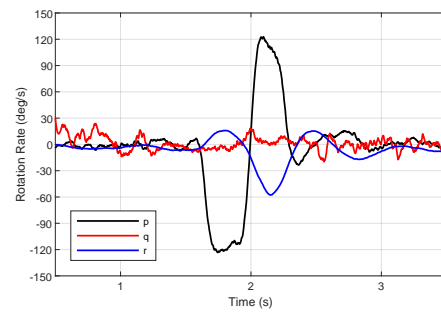
(**b**) Rotation rate responses for doublet #1.
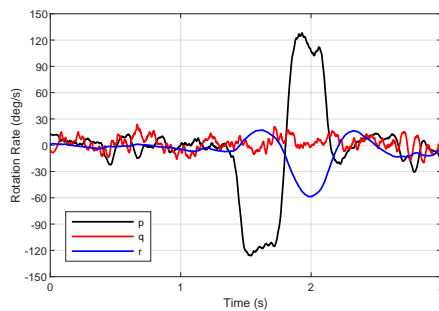
(**c**) Rotation rate responses for doublet #2.

(**d**) Rotation rate responses for doublet #3.

Figure 5. The (**a**) control input and (**b**–**d**) rotation rate response time history for 3 automated aileron doublets; note that (**b**) is the response for input (**a**) and that (**c**,**d**) are responses for inputs with identical square waves as (**a**) that are slightly time shifted.

3.2. Measurement

Knowledge of aircraft parameters, including geometric, inertial, and subcomponent properties, is vital in the analysis of flight testing results. Traditionally, for full-scale, manned aviation, aircraft developers and modifiers have complete knowledge of these aircraft parameters as it is required for aircraft certification purposes. However, in the case of UAV development, developers, especially researchers, often use existing COTS airframes that have limited parameters available. A review by Sobron et al. of research platforms between 2010 and 2020 showed that at least 18 of the aircraft surveyed were developed from COTS airframes [81]. Beyond the scope of the aforementioned review, commercial (closed-design) airframes such as the UAV Factory Penguin airframe have been used as a basis by over 20 research institutions since 2010 with similarly limited parameters available [82]. Therefore, to accurately create or update an aircraft model, several measurement methods were either developed or adapted to support the UAV Development Framework, including 3D aircraft scanning, moment of inertia measurement, and propeller testing [56]. The following two sub-sections describe these novel methodologies that allow a user to accurately measure aircraft geometry and moment of inertia.

3.2.1. 3D Scanning

Utilizing an existing commercial airframe in the development of a UAV comes with the challenges of unknown geometry. Knowledge of the aircraft geometry is paramount when attempting to implement the aircraft in an aerodynamic analysis tool or a flight simulation software. The contemporary method to measure this geometry has been the manual measurement of aircraft dimensions, which often includes the estimation of complex curves [12,64,83]. Thus, a 3D scanning and analysis methodology was developed, which allows the user to scan an uncharacterized aircraft of any size [84]. The point cloud generated by the 3D scan is then processed to produce detailed geometry of the aircraft, output either as a computer-aided design (CAD) file or as a set of geometric parameters.

A 3D scanning demonstration was performed using the Avistar UAV. The demonstration was performed using a ZCorporation ZScanner 800 self-positioning handheld 3D scanner [85]. Figure 6 shows a photo of the Avistar UAV as it is being scanned. The 3D point cloud output from the scanner was processed using a MATLAB script called AirplaneScan that rotated, translated, and aligned it to its principal axes as well as allowed for mirroring about the central plane. The processed point cloud was then sliced multiple times to yield the cross-sections of the fuselage, wings, and tail sections. These point cloud slices provided dimensions and coordinates for all of the flight and control surfaces. The wing airfoil coordinates were verified with coordinates for the AVISTAR airfoil found on the UIUC Airfoil Database [86] and the stabilizer airfoils were verified with manual measurements. Using the fuselage geometry from the 3D scan and the aforementioned flight surface geometry values, a CAD model of the aircraft was made in SolidWorks, as seen in Figure 7.

The resulting geometry data and CAD model were used to develop a flight model in the X-Plane flight simulator as part of the emulation environment presented in Section 3.3.1; a screenshot is shown in Figure 8. Additionally, the geometry was to compute the aircraft's aerodynamic characteristics using several computational tools of varying order: the lifting-line theory aerodynamic tools, XFLR5 and AVL, and the computational fluid dynamics (CFD) tool Ansys Fluent; these computed aerodynamic characteristic values were then compared to values estimated from flight testing data [87]. Recently, similar methodology has been used by other researchers [88].

Figure 6. The 3D scanning of the Avistar UAV with the ZScanner 800.
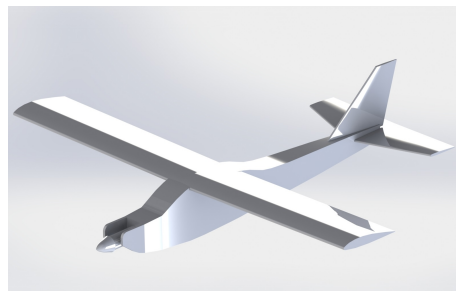
Figure 7. The SolidWorks CAD model of the Avistar UAV.

Figure 8. The X-Plane flight model of the Avistar UAV.

3.2.2. Moment of Inertia

Knowledge of moment of inertia data for an aircraft is critical for both aerodynamic analysis as well as model development for control, all integral components of the UAV Development Framework. There have been a variety of different methods employed to measure the moment of inertia, including physical pendulums, bifilar pendulums, compound pendulums, torsional pendulums, and torque [89–97]. The accuracy of the inertias determined using these methods depend upon a variety of factors, such as friction, drag, and vibrations. These contributions can be significant, as errors due to drag can increase quadratically depending upon how fast the inertias are being measured, and friction can increase as mass is added to the system.

In recent work, Jardin and Mueller developed a bifilar pendulum that accounts for both damping and air resistance with accurate results for small inertia values; however, errors of 12% occurred from the measurements as the mass and area of the measured object increased (to the size of a small/medium-sized UAV), requiring additional mass corrections [94]. Bowman developed a knife-edge pendulum, which yielded low errors for small aircraft yet generated errors as high as 40% for larger UAVs [95]. Lehmkuhler et al. examined moment of inertia testing in detail and developed two types of physical pendulum testing methods: single degree-of-freedom and three degree-of-freedom [97]. The testing methods take into account geometric-based corrections for drag to increase accuracy. These corrections, which can account for up to 25% of the values, were based on results from testing an aircraft-shaped flat plate and a foam-simulation aircraft. Using the corrections, the testing methods yielded errors between 0 and 3.3% for the single degree-of-freedom tests and errors between 0 and 13.6% for the three degree-of-freedom tests.

The methods in the literature provide a range of testing options but are, for the most part, rather time-intensive in their implementation and troublesome in terms of minimizing error. This provided the motivation to develop a moment of inertia testing method that would be both quick and easy to use as well as insensitive to external factors, thereby minimizing potential sources for error. Taking inspiration from motor-driven, torque-based moment of inertia testing rigs used to measure micro- and cube satellites, a known-mass and pulley, torque-based moment of inertia testing rig was developed [57]. The rig is intended for small to medium-sized UAVs and is made up of three functional elements: a $1.2 \times 1.2 \times 1.8$ m ($4 \times 6 \times 6$ ft) steel framework, a rotation assembly, and a 100 Hz instrumentation system. The moments of inertia are determined by applying a known torque using a known mass to the pulley system, which will cause the system to accelerate.

Validation was performed on the moment of inertia testing rig using two types of calibration piece: plastic and steel bars with high inertia and low drag and an MDF flat plate with low inertia and high drag. In both cases, the results showed that the rig is able to very accurately measure the moment of inertia of an object, i.e., within 5%. For the MDF flat plate, angular velocity data measurements showed that total drag, assuming a drag coefficient of 1.98 [98], averaged to 0.257% of the torque applied to the pulley and, as such, is significantly smaller than the torque applied through the pulley; thus, it can be disregarded.

Thus far, the moment of inertia testing rig has been used to test two UAVs: the Avistar UAV (shown in Figure 9) and a Cirrus SR-22T (an approximately 1/5 scale model used as a distributed electric propulsion testbed [99]). Both of these aircraft were mounted into the rig using various methods and tested on all 3 axes.

Figure 9. Roll moment of inertia testing of the flight-ready Avistar UAV testbed.

3.3. Modeling and Emulation

In order to decrease development time, modeling and emulation have become an important component of the UAV Development Framework. Instead of prototyping, testing, and analyzing through the many stages of aircraft development in hardware, which are resource- and time-intensive, a virtual aircraft and its sub-systems are modeled and then implemented in the emulation environment, i.e., creating a "*Virtual Twin*". The *uavEE* emulation environment integrates a high-fidelity simulator with layers of modeling (e.g., a power consumption model), flight control software (e.g., autopilot software), and interfaces to hardware components (e.g., flight control board and sensors). Therefore, the UAV Development Framework enables virtual design iterations for both new and existing aircraft and sub-system designs.

3.3.1. Modular Emulation Environment

uavEE was developed to provide a modular emulation environment where a user can test a broad range of aircraft systems in a virtual environment, piece-wise or holistically [100]. The environment starts by creating a real-time connection between a high-fidelity flight simulator (e.g., X-Plane or FS One) and an autopilot software, and then modeling layers are introduced, allowing for additional emulation complexity. Therefore, the physical aircraft design, the software, the flight computation, and possibly payloads can be tested in the lab.

In the flight simulator, an aircraft design of interest can relatively easily be created using the included simulator tools. However, the user may choose to use an existing aircraft design if that is not the effort of interest (e.g., using the full-scale Cessna 182 in X-Plane to develop the flight testing automation process). Likewise, the autopilot software being tested can be completely new or from an existing project/base with possible modifications being made. The software can either be run on the desktop machine or from an external machine, i.e., an embedded board connected to the simulator environment through an interface. This design therefore affords the user the ability to separately focus on different parts of hardware and software development and integration.

Thus, within the scope of software development, the emulation environment allows for a step-wise software prototyping process that allows the user of uavEE to first focus on the software development and testing, followed by avionics hardware integration and emulation, drastically improving debugging efforts as compared to traditional development work. As the development and testing of avionics for UAVs is an iterative process that involves many flight tests and multiple revisions of software and hardware, quick deployment in uavEE has been shown to save hours in the field, dramatically increasing the success rate of actual flight tests.

A system diagram of uavEE is shown in Figure 10. The uavEE emulation environment typically consists of embedded flight control hardware, the uavGS ground station running on a Linux computer, and a simulator. A uavEE plugin in the simulator, X-Plane 11 [53], collects the sensor data from the simulation, sending it to the emulation interface. It further translates received actuation packets from the emulation interface into control commands in the flight simulator. Yellow components are used only during real flight and are disconnected during emulation, while blue components are only used in emulation and disconnected in real flight. Components that are green are used at all times, during real flight and in emulation. uavEE provides reliable sensing and actuation to travel between the autopilot and the flight simulator through in-memory or ethernet communication. The modular ground control interface, uavGS, shown in Figure 11, is used to command and monitor the aircraft autopilot in both emulation as well as in real flight. The ground station interface is the product of a multi-year evolution, starting in 2014.
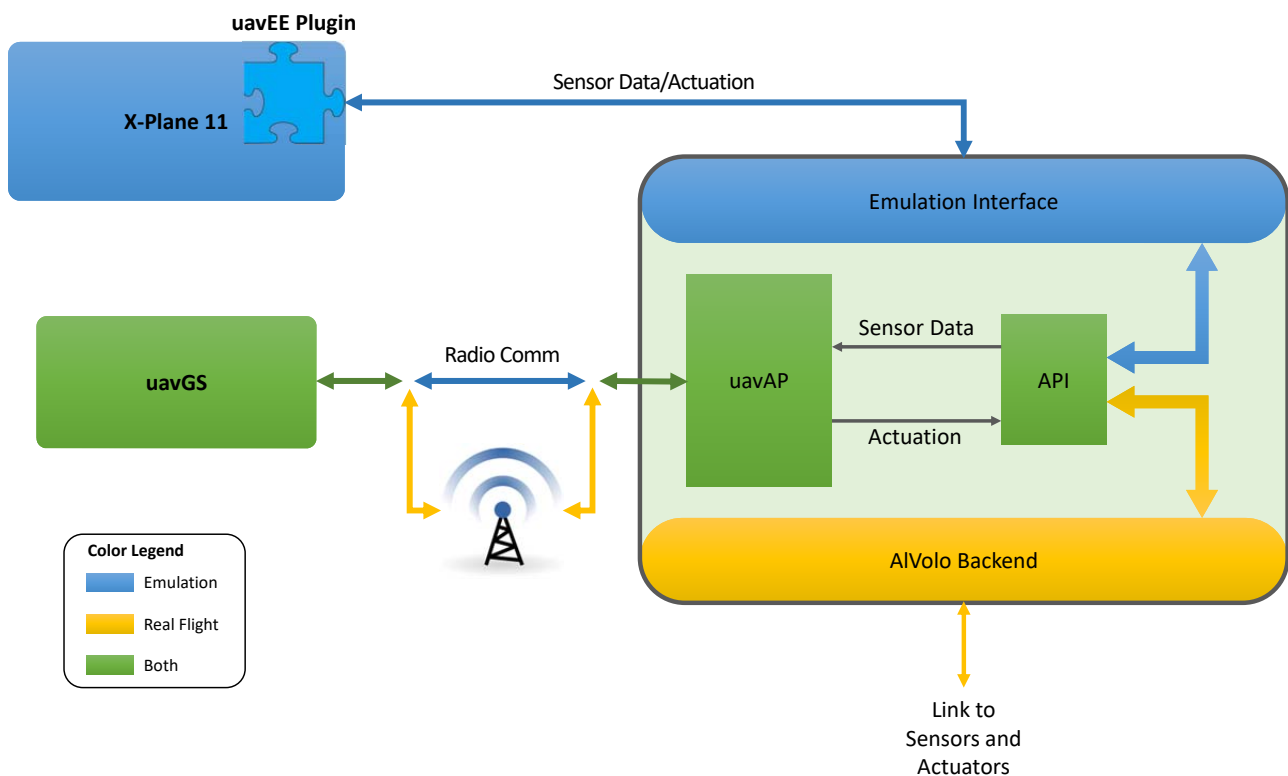
Figure 10. A system diagram of uavEE in emulation and real flight.
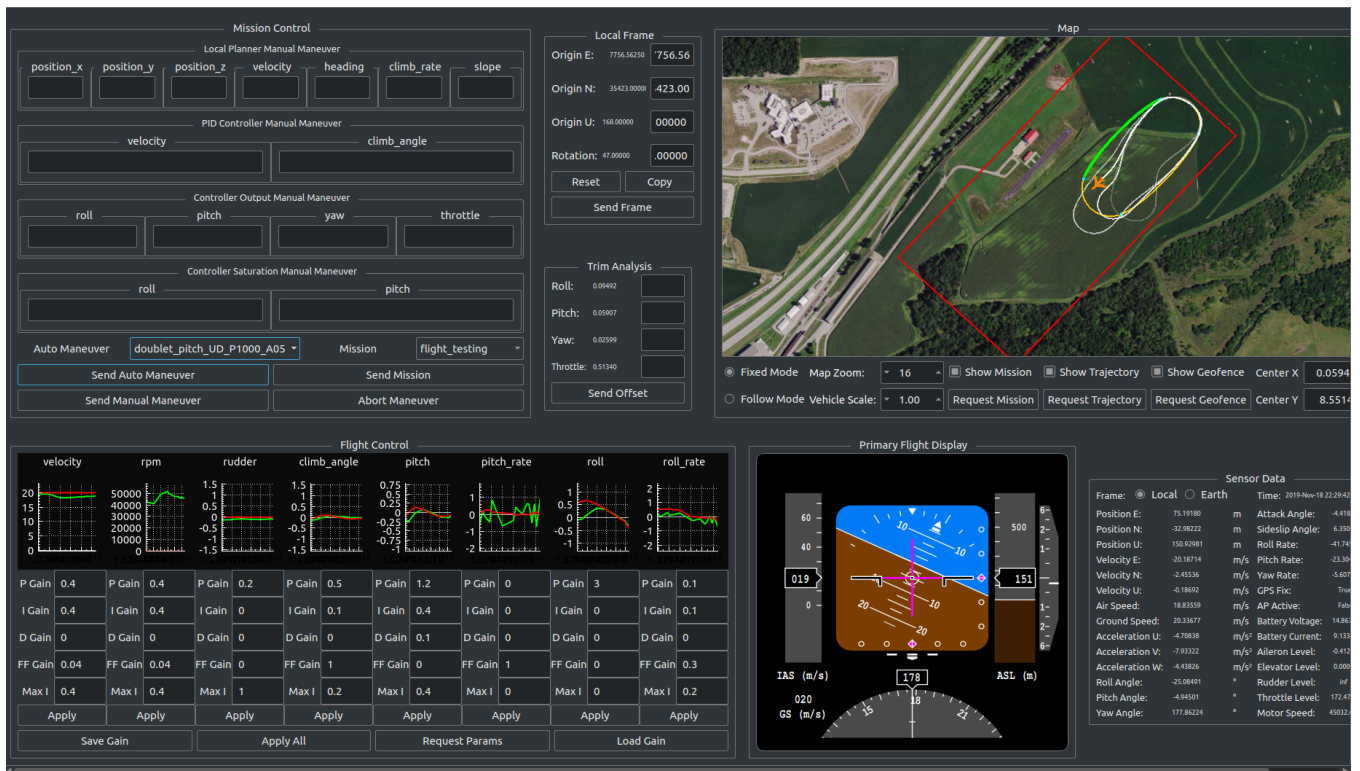
Figure 11. The uavEE ground station interface, which provides functionality in emulation and real flight; it is shown being used to automate a pitch doublet maneuver as part of the flight testing automation process.

Modeling layers can be introduced into the uavEE plugin to provide additional capability. Currently, modeling layers that have been introduced include a propulsion system consumption model and an aircraft fault model. The propulsion system consumption model, which has been shown to provide very accurate estimation, will be discussed in more detail in the following sub-section; it is of particular interest as the propulsion system of a typical electric UAV consumes more than half of the available energy. Therefore, optimizing the propulsion system, which is discussed in Section 3.4.1, is especially important for aircraft with strict power budgets, such as solar-powered UAVs, discussed in Section 4. Currently, a second modeling layer, the aircraft fault model, is in development to trigger aircraft sub-system failures such as engine loss [101]. It is also currently of interest to add a network protocol modeling layer as it is critical for multi-agent communication and control [102].

3.3.2. Electric Aircraft Power Consumption Model

A high-fidelity, low-order power model for electric, fixed-wing UAVs was developed [52] and subsequently integrated into the uavEE emulation environment and the propulsion system component optimization tool. Previous works have separately looked at aircraft power modeling [103–108] and propulsion system modeling [109–113] with varying degrees of assumptions and verification. Compared to existing works, the propulsion power model developed provides a more holistic approach to UAV propulsion power modeling and has been tested under realistic flight conditions (described below).

The power model uses propulsion modeling of the propeller and motor as well as aircraft modeling using flight mechanics derivations. In order to enable online computation with limited resources, the resulting expression has been limited to using only measurable aircraft state variables, propulsion system parameters and curves, and (scalar) constants.

The final expression for the developed power model is:

$$P_{propulsion} = K_p \frac{v^3}{\eta_p \eta_m} + K_i \frac{\cos^2 \gamma}{\eta_p \eta_m v \cos^2 \phi} + mg \frac{v \sin \gamma}{\eta_p \eta_m} + m \frac{\vec{a} \cdot \vec{v}}{\eta_p \eta_m} \tag{1}$$

where η_p is the propeller efficiency, η_m is the motor efficiency, and K_p and K_i are scalar constants. These scalar constants can be determined from aircraft specifications, per the expressions below, or can be learned through linear regression using a training dataset. The expressions for these scalars are

$$K_p = \frac{1}{2} \rho S C_{D_o} \tag{2}$$

$$K_i = \frac{2Km^2g^2}{\rho S}. \tag{3}$$

The propeller efficiency can be derived using blade element momentum theory (BEMT) and sectional airfoil theory as done in [114]. However, BEMT curves are highly sensitive to variations in the parameters used. In order to increase model accuracy, experimental data for propeller performance can be obtained from wind tunnel propeller testing and/or an existing database [115], with interpolation being done as required. This latter technique is in use.

The motor efficiency for a brushless DC-motor can be calculated analytically using the relation between motor terminal voltage U_m and shaft rotation rate Ω and a variety of fixed motor parameters. A first-order approximation [116] is given as

$$\eta_m(\Omega, U_m) = \left(1 - \frac{i_0 R}{U_m - \Omega/K_v} \right) \frac{\Omega}{U_m K_v}, \tag{4}$$

where i_0 is motor current at zero load, R is motor internal resistance, and K_v is motor speed constant. A second-order approximation [117] can be used; however, it requires additional data, which are not easily obtained from motor manufacturers and need to be measured by the user through benchtop testing [118].

The resulting power model was evaluated by means of flight testing using the high-fidelity flight control and data acquisition system described in Section 3.1.1. By flying the Avistar UAV through a reference flight path, which contained turns, climbs, descents, and straight-line segments, the results showed very close agreement between the power and energy estimates determined using the power model from aircraft state data and actual experimental power and energy measurements. Additionally, using the emulation environment, the reference flight path was also flown using the same autopilot and a simulated radio control model aircraft trainer, which was very similar to the one used in experimental flight testing. These flight paths are displayed in Figure 12. The flight path was nearly identical with the exception of 2 corners, where, in experimental flight testing, light wind gusts deviated the aircraft slightly. The power and energy data generated were in close agreement with the experimental data, as can be seen in Figure 13. The significance of this result is that the propulsion power model that was developed is able to accurately estimate the power consumption of an electric UAV based on flight path state without needing precise aerodynamic measurements or estimation, e.g., angle-of-attack. Therefore, power estimation can be done with minimal computation.
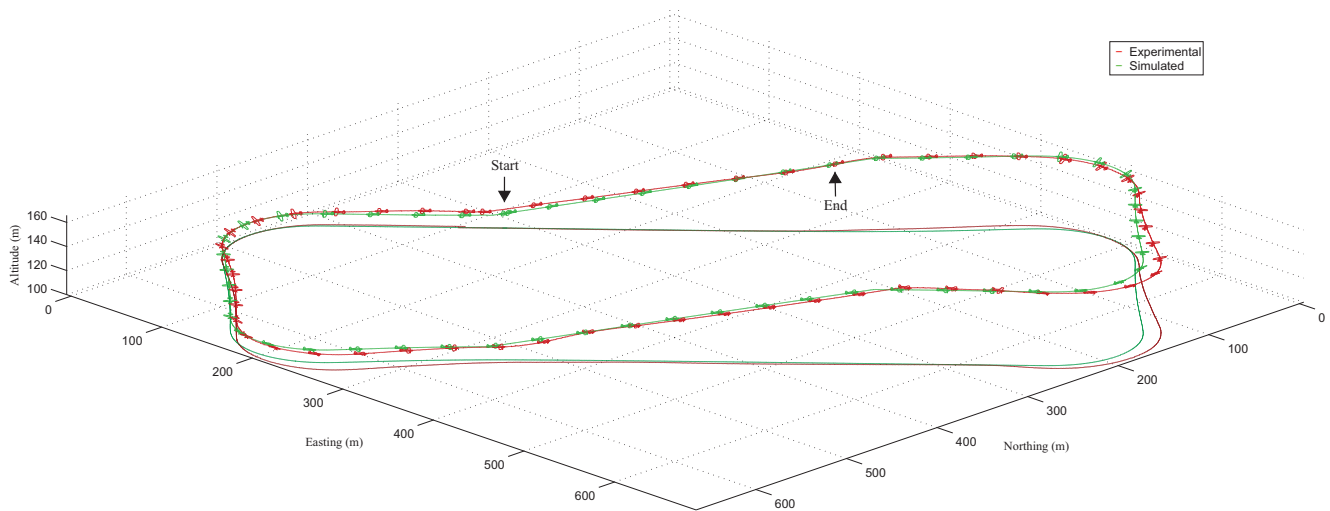
Figure 12. Comparison of aircraft path for experimental (red) and simulated flight (green) results; the aircraft is plotted every 2 s.
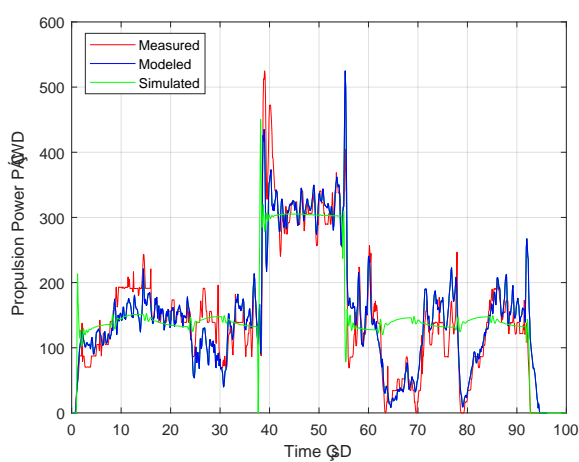
(**a**)
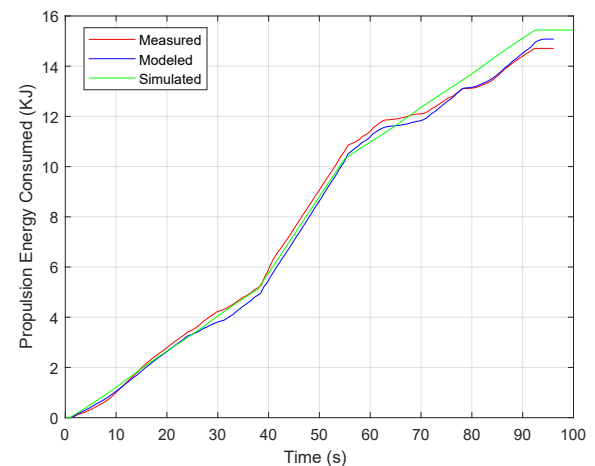
(**b**)

Figure 13. Comparison of (**a**) propulsion power and (**b**) energy consumed from experimental measured (red), experimental modeled (blue), and simulated (green) results using the propulsion power model.

3.4. Optimization

Optimization is a key driver of the aircraft development process, which is especially true within the UAV Development Framework. Optimization drives the evolution of an aircraft or aircraft system, whether it be directly through its design or indirectly in terms of its requirements. The most common form of optimization in contemporary aircraft design is a trade study. The UAV Development Framework not only allows for trade studies to be performed but also for other types of optimization techniques. Currently, as the focus application of the UAV Development Framework is high-efficiency, electric-powered flight, the Propulsion System Optimization Tool was developed and integrated into the framework.

3.4.1. Propulsion System Optimization Tool

Limited onboard energy storage significantly limits flight time and, ultimately, the usability of UAVs. The propulsion system plays a critical part in the overall energy consumption of the UAV. Therefore, it is necessary to determine the most optimal combination of possible propulsion system components for a given mission profile, i.e., propellers,

motors, and electronic speed controllers (ESCs). Hundreds of options are available for each of the components, with generally non-scientific advice for choosing the proper combinations. To date, there has been significant effort in the modeling [119–122] and testing [111,112,118,123–134] of UAV propulsion system components. However, there has been comparatively limited effort put into optimizing the matching of these components [135], with most of the effort towards custom-designed or generic-shaped propellers [50,136–139].

The Propulsion System Optimization Tool [51] was developed that determines (matches) the optimal propeller and motor combination(s) for an electric, fixed-wing UAV, given desired mission requirements, i.e., it determines the combination(s) that provide the required thrust at the greatest operational efficiency, i.e., using the least amount of energy. Specifically, mission profiles are broken down into expected segments, with velocity and thrust requirements being computed using an aircraft power model. The optimization tool then estimates the required propeller rotation rate and then power consumption for each segment and propeller–motor combination. It then integrates the segment results into missions for each combination and tabulates the results, sorted by overall efficiency. Figures 14 and 15 present process diagrams that explain how the propulsion optimization occurs. Among a variety of additional functionality integrated into the tool, the optimizer considers aircraft safety by estimating the maximum thrust each combination can produce, which is crucial in upset recovery scenarios such as stall.
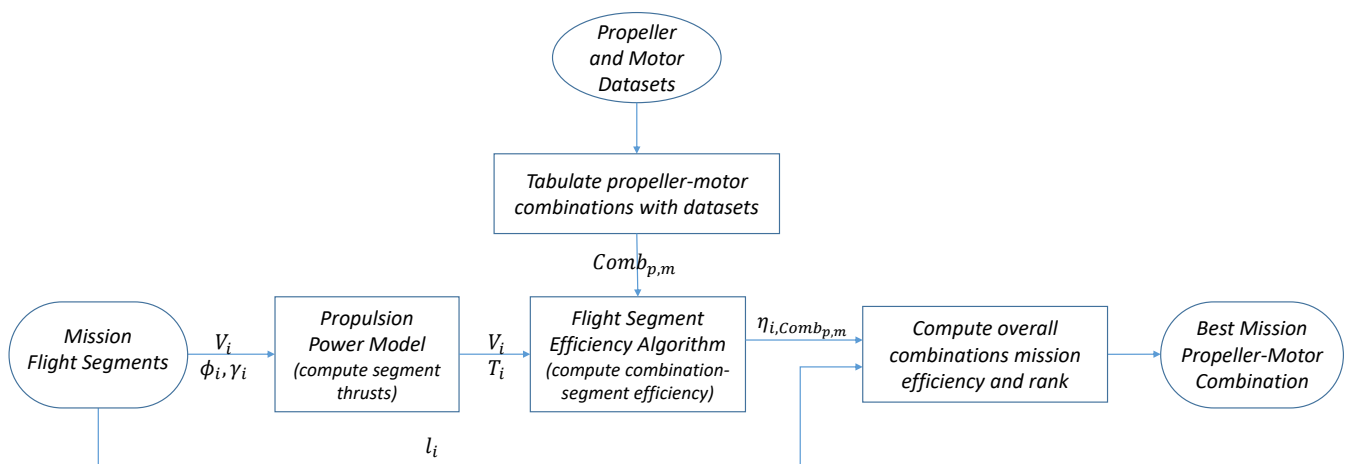

Figure 14. Process diagram for the *Mission-Based Propulsion System Optimization*.
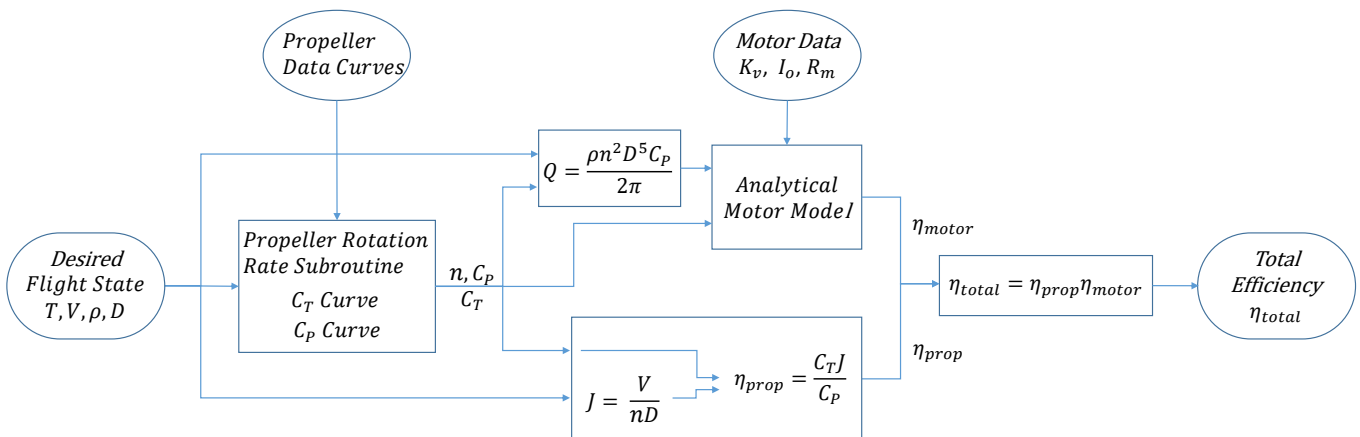

Figure 15. Process diagram of the *Flight Segment Propeller–Motor Efficiency Algorithm*.

Experimental validation testing of the optimization tool was performed through flight testing of the Avistar UAV. Due to practical limitations, the validation testing used the

existing aircraft motor, the AXI 4120/14, and a choice of APC propeller [140] as they are readily available, low-cost, and have been previously performance tested [115]. The optimization tool was then applied to determine the combination(s) that would be the most efficient in 20 m/s level flight, assuming a thrust requirement of 3, 4, or 5 N (the estimated required thrust). The results presented in Figure 16, show 6 propellers that provide greater efficiency than the default propeller, the APC 13 × 8 E; however, only one, the APC 11 × 10 E, provides sufficient thrust available at the stall speed of the test aircraft for a reasonable margin of safety in flight testing. Thus, the aircraft was manually piloted in straight and level flight at approximately 20 m/s with the AXI 4120/14 motor and the APC 13 × 8 E and APC 11 × 10 E, respectively. The results showed that the optimized combination requires approximately ***20% less power*** than the default combination.


(**a**)

(**b**)
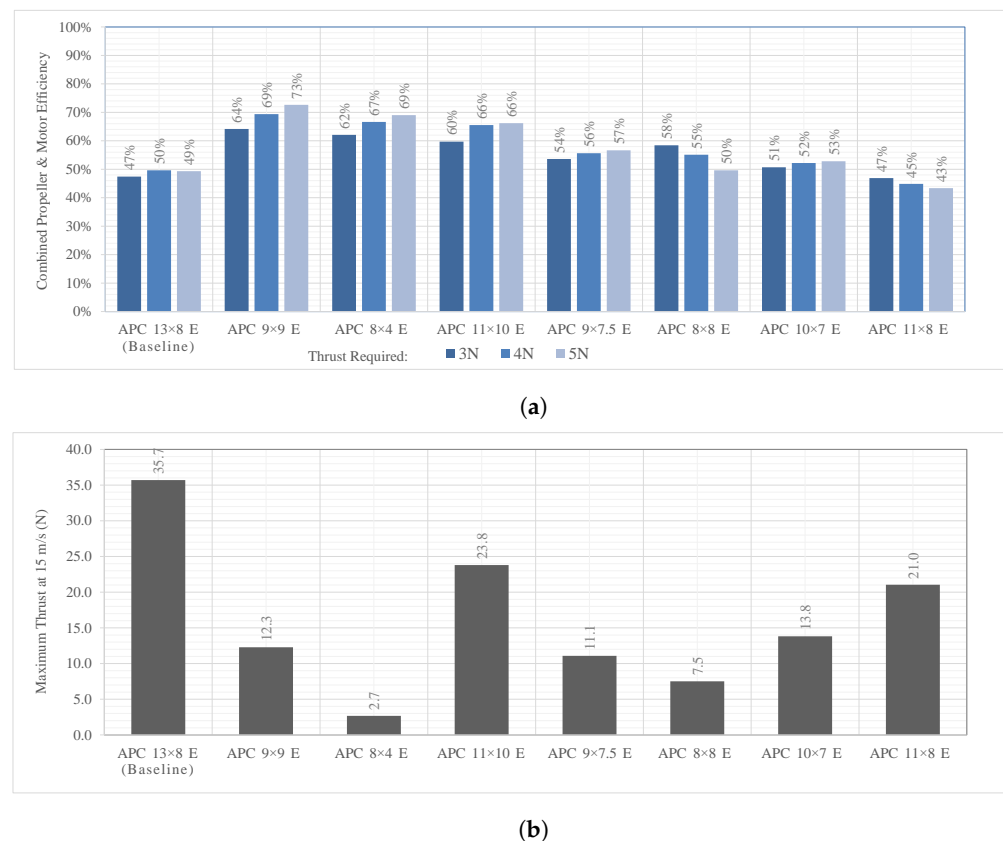
Figure 16. Comparison of (**a**) motor propeller efficiency for required thrusts of 3, 4, and 5 N at 20 m/s and (**b**) the maximum thrust available at 15 m/s for AXI 4120/14 motor with various APC E propellers.

Additionally, propulsion system optimization of potential missions was performed in simulation. The simulated missions, which included a 1 km by 1 km field coverage flight (described in Section 4) and a 6-site inspection flight about an 8 km^2 area, showed the advantage of using mission optimized propeller–motor combinations with significant efficiency gains of ***50% to 75%*** relative to the default combination. Performing this propulsion system optimization is especially paramount for long-endurance and/or solar-powered aircraft.

4. Framework Demonstration

To demonstrate the framework, an example application was performed with a mixture of virtual and real-life testing: to quickly develop an unmanned aircraft for agricultural field surveillance. Agricultural applications, as well as many other applications previously mentioned, require UAVs to perform path following, often for coverage of a predefined area. The UAV Development Framework is therefore applied to quickly develop an aircraft for agricultural coverage path planning. First, the general methodology is applied, followed by a mission-specific methodology. Figure 17 graphically shows the application of the

UAV Development Framework to the agricultural mission with the orange dashed lines denoting the general methodology that is first applied and the dark navy blue dashed lines denoting the mission-specific methodology that is subsequently applied.
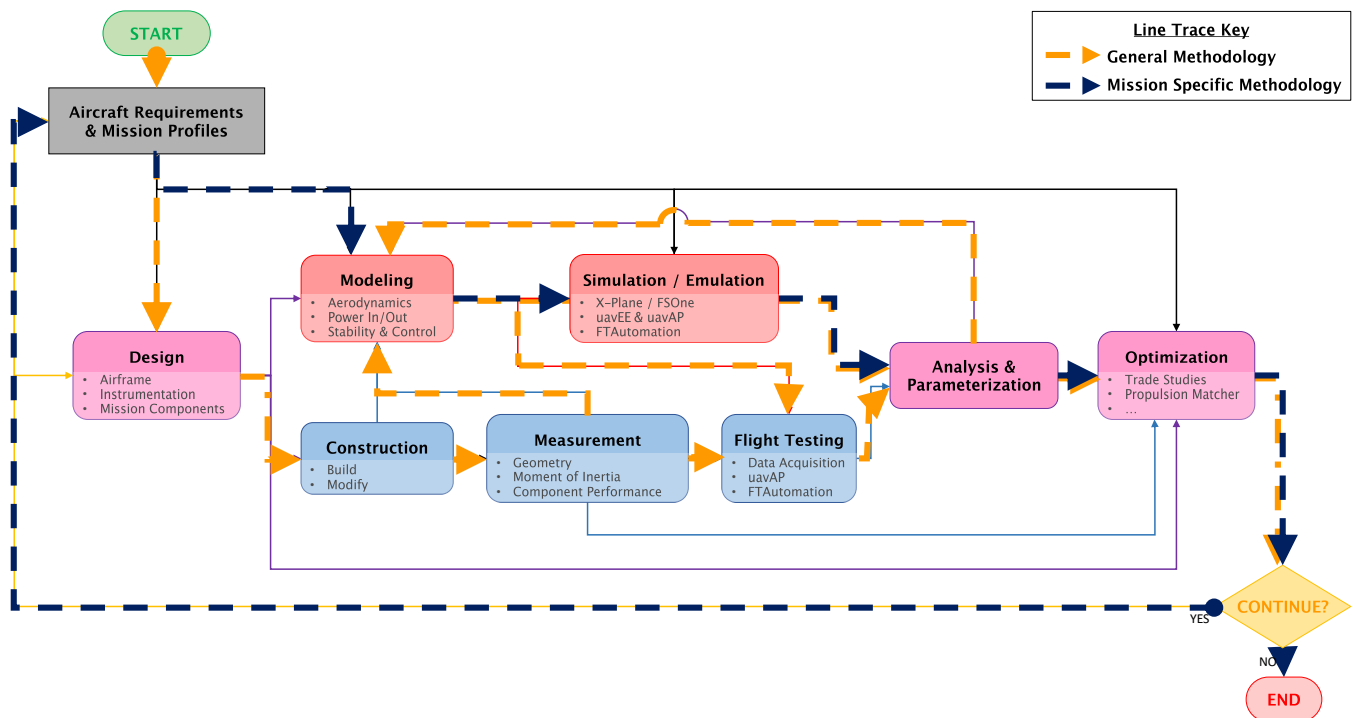
Figure 17. The UAV Development Framework used to quickly develop an aircraft for agricultural field surveillance.

4.1. General Methodology

Application of the UAV Development Framework for the general coverage path planning mission begins with defining *Aircraft Requirements & Mission Profiles*. As the aforementioned Avistar UAV trainer airframe is capable of fulfilling coverage path planning, it is used for this example and therefore yields the aircraft *Design*. Thus, the Avistar UAV aircraft undergoes *Construction* with building or modifying as needed. Afterward, the aircraft undergoes *Measurement*, including geometric measurement using 3D scanning, moment of inertia measurement, and component performance measurement (e.g., propulsion system component testing); these measurement techniques were described for the Avistar UAV earlier in Section 3.2. The results from *Measurement* are then used for *Modeling*. In parallel to *Modeling*, *Flight Testing* is performed using the *DAQ*, *uavAP*, and *Flight Testing Automation*, as previously presented in Section 3.1. The flight testing results allow the aircraft's flight performance to be *Analyzed & Parameterized*, which are fed back into *Modeling*.

For example, the *Electric Aircraft Power Consumption Model* uses data collected through propulsion testing of the aircraft motor and propeller (during *Measurement*) as well as aircraft efficiency data gathered through *Flight Testing* and subsequent *Analysis & Parameterization*. Other information such as *Geometry* and *Moment of Inertia* and control response measurements are also used to develop the aircraft *Model*, which is then implemented into the *X-Plane* simulation model in *uavEE*. Note that aircraft control derivatives are attained through *Flight Testing Automation*. This data collection loop iterates as additional information is collected.

4.2. Mission-Specific Methodology

The UAV Development Framework is then applied to a specific example mission profile, a 1 km by 1 km field coverage inspection flight, which is typical for agricultural applications. A trajectory plot of the mission is presented in Figure 18. The mission begins

with a takeoff followed by a 15 degree climb to 50 m in altitude. The aircraft then turns toward the desired area and flies straight for approximately 400 m. It then maneuvers and proceeds to fly a zig-zag field coverage with 50 m radius turn-arounds after each pass. The field is covered after 11 passes, at which point the aircraft flies back toward the runway, maneuvers, and finally descends. The entire mission is flown at 20 m/s except for the climb out after takeoff and descent to landing. For the example mission, it is assumed that the aircraft requirements include a mission sensor, which, for brevity's sake, is modeled as a constant power sink. Furthermore, the aircraft needs to be able to satisfy the mission requirements with the least possible development effort (time and resources).

As the Avistar UAV aircraft has already been selected for this mission, further aircraft development done using the UAV Development Framework involves propulsion system optimization to increase the energy available to the mission sensor and increase flight time. Within the framework, the process starts at *Aircraft Requirements & Mission Profiles*, where the specific requirements have just been specified for the example field coverage mission. The process then proceeds towards *Modeling*. The *Electric Aircraft Power Consumption Model* is implemented in the *uavEE* emulation environment using *X-Plane*, allowing for a simulation of the mission to occur, with power consumption being estimated for the Avistar UAV aircraft. The energy consumed is then computed through *Analysis & Parameterization*.

If the energy required is less than the energy available, one could pass through *Optimization* without the need for further effort toward the end step of the framework. However, if the energy required is greater than the energy available, one could use the *Propulsion System Optimization Tool* within the *Optimization* block to determine if a better-matched motor and propeller combination could enable the mission. If the *Optimization* yields a significant enough decrease in energy consumption, one could proceed towards the end; if not, further *Design* considerations should be made in the next iteration.
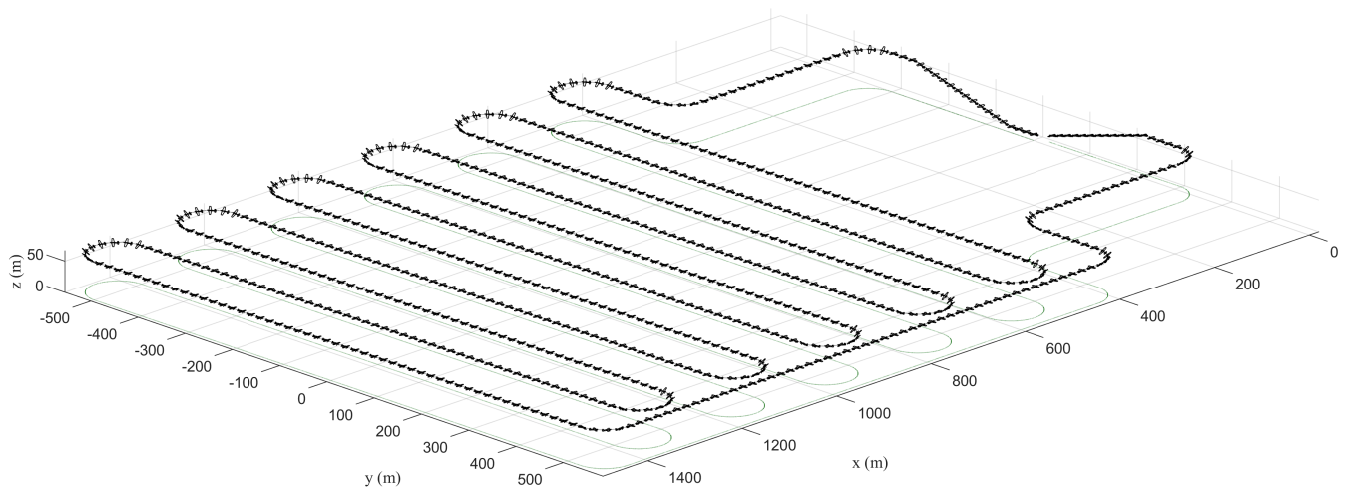
Figure 18. Trajectory plot of the simulated 1 km by 1 km field coverage flight mission (the aircraft is plotted $8\times$ scale every 1.0 s).

Assuming that propulsion optimization needs to be performed, thrust requirement predictions are generated by the *Electric Aircraft Power Consumption Model*. The velocity and thrust profiles are then fed into the *Propulsion System Optimization Tool* with a list of potential motors and propellers that could be feasibly used on the aircraft. The Propulsion System Optimization Tool produces a table of over 1300 potential combinations along with estimated input energy consumption, overall-average efficiency, and maximum thrust at the minimum speed (estimated stall speed) of 15 m/s. Table 1 presents the 10 most efficient propeller–motor combinations, as well as the baseline combination that was ranked 410, and their respective performance estimates for the field coverage mission. As can be seen from the table, there is a significant ∼50% relative improvement in efficiency, from 49.6% for the baseline propeller and motor combination to ≥74% for the top 7 propeller–motor

combinations. However, as is expected, there is a reduction in maximum thrust at the minimum speed of 15 m/s for the most efficient propeller–motor combinations compared to the baseline combination. Due to this decrease, one would choose the 3rd or 4th ranked combination as it likely offers sufficient, safe maximum thrust at the minimum speed of 15 m/s. The Avistar UAV would then be able to perform the field coverage inspection flight using 33% less power, which could be allocated to other onboard devices.

Table 1. The propulsion system optimization results sorted by efficiency for the simulated 1 km by 1 km field coverage mission; note that combinations with insufficient thrust at minimum speed are crossed out (struck through), the most efficient combinations with sufficient thrust at minimum speed are highlighted in green, and the baseline combination is highlighted in yellow.

Ranking	Propeller	Motor	Total Energy (J)	Average Efficiency (%)	Maximum Thrust (N)
1	~~APC 9 × 9 E~~	~~Hacker A40-10S V4~~	87,614	74.7	16.3
2	~~APC 9 × 9 E~~	~~Hacker A40-14L V4~~	87,657	74.7	2.6
3	APC 9 × 9 E	Neu 1512/5.5D	88,113	74.3	23.8
4	APC 9 × 9 E	Neu 1512/5D	88,303	74.1	28.8
5	~~APC 9 × 9 E~~	~~Hacker A40-10L V4~~	88,400	74.0	6.5
6	~~APC 9 × 9 E~~	~~Hacker A40-12L V4~~	88,408	74.0	4.0
7	APC 9 × 9 E	Neu 1512/5.75D	88,436	74.0	21.8
8	APC 9 × 9 E	Neu 1512/5.25D	88,540	73.9	26.0
9	~~APC 9 × 9 E~~	~~Neu 1512/6D~~	88,709	73.8	19.9
10	~~APC 9 × 9 E~~	~~Hacker A40-14S V4~~	89,023	73.5	7.4
410	APC 13 × 8 E	AXi 4120/14	132,047	49.6	35.7

5. Conclusions

The current paper presents a cyber-physical prototyping and testing framework to enable the rapid development of UAVs called the UAV Development Framework. The framework is an extension of the typical iterative engineering design and development process, specifically applied to the rapid development of fixed-wing UAVs. Unlike other development frameworks in the literature, the framework allows for iteration throughout the entire development process from design to construction, using a mixture of simulated and real-life testing as well as cross-aircraft development. For specific aircraft or application requirements, methods and tools can be added, removed, or modified as need be within the framework.

The framework presented includes low- and high-order methods and tools that can be applied to a broad range of fixed-wing UAVs and can either be combined and run simultaneously or be run sequentially. As part of this work, seven novel and enhanced methods and tools were developed in the areas of flight testing, measurement, emulation and modeling, and optimization. These methods and tools include (1) data acquisition, (2) flight testing automation, (3) 3D scanning, (4) moment of inertia measurement, (5) modular emulation, (6) electric aircraft power consumption modeling, and (7) propulsion system optimization. However, the framework could also be applied to a variety of aircraft types, e.g., fuel-powered, rotary-wing aircraft, or multi-rotors, with the inclusion of methods and tools that are suited for those architectures.

Finally, a demonstration of the UAV Development Framework was presented. The demonstration showed how to quickly develop an unmanned aircraft for agricultural field surveillance based on an existing platform, with general and mission-specific methodology.

6. Future Work

Since the inception of unmanned aircraft, a key design driver and limiter has been the limited onboard energy storage, as it significantly constrains flight time and, ultimately, usability. A major technical hurdle to overcome is that of drastically reducing the overall

power consumption of a long-endurance UAV so that it can be powered by solar arrays, therefore extending flight time. When powered by solar arrays, a careful reduction in battery size can decrease the aircraft's weight, reducing propulsion power even further. An additional advantage of long-endurance flight is the increase in aircraft availability and the decrease in takeoffs and landings that constitute the riskiest portions of flight. Currently, all long-endurance solar-powered aircraft have incorporated custom airframe designs and many custom components (e.g., single-application propellers and gearboxes, maximum peak power-point trackers, etc.) [141,142]. However, to truly enable many applications, solar-powered aircraft need to be assembled from only commercial off-the-shelf (COTS) components as well as sustain continuous flight. Using only COTS components reduces aircraft cost, thereby increasing accessibility to the community.

With these goals in mind, the UAV Development Framework is being used to develop a computationally intensive, long-endurance solar-powered unmanned aircraft, which is called the UIUC-TUM Solar Flyer [143]. As with the example application presented in this paper, the development of the solar-powered aircraft requires multiple iterations from conception to flight demonstration of the desired aircraft capabilities. A comparison of the developed solar unmanned aircraft to a similar aircraft developed using a different methodology can be performed to compare the development timeline and resource requirements.

Author Contributions: Conceptualization, O.D.D. and M.C.; methodology, hardware, and analysis, O.D.D.; software and validation, M.T. and O.D.D.; writing—original draft preparation, O.D.D.; writing—review and editing, O.D.D., M.T. and M.C.; supervision, M.C.; project administration, O.D.D. and M.C.; funding acquisition, M.C. All authors have read and agreed to the published version of the manuscript.

Data Availability Statement: Not applicable.

Conflicts of Interest: The authors declare no conflict of interest.

Abbreviations

The following abbreviations are used in this manuscript:

ADC	analog-to-digital converter
BEMT	blade element momentum theory
CAD	computer-aided design
CFD	computational fluid dynamics
COTS	commercial off-the-shelf
DAQ	data acquisition
ESC	electronic speed controller
GPS	global position system
IMU	inertial measurement unit
I/O	input/output
MDA	multi-discipline analysis
MDO	multi-discipline optimization
PWM	pulse width modulation
UAV	unmanned aerial vehicle
VLOS	visual line-of-sight

References

1. Federal Aviation Administration. Integration of Civil Unmanned Aircraft Systems (UAS) in the National Airspace System (NAS) Roadmap, 2nd ed. 2018. Available online: https://www.faa.gov/uas/resources/policy_library/media/Second_Edition_Integration_of_Civil_UAS_NAS_Roadmap_July%202018.pdf (accessed on 31 January 2022).
2. Lykins, R.; Keshmiri, S. Modal Analysis of 1/3-Scale Yak-54 Aircraft Through Simulation and Flight Testing. In Proceedings of the AIAA Paper 2011-6443, AIAA Atmospheric Flight Mechanics Conference, Portland, OR, USA, 8–11 August 2011. [CrossRef]
3. Johnson, B.; Lind, R. Characterizing Wing Rock with Variations in Size and Configuration of Vertical Tail. *J. Aircr.* **2010**, *47*, 567–576. [CrossRef]
4. Perry, J.; Mohamed, A.; Johnson, B.; Lind, R. Estimating Angle of Attack and Sideslip Under High Dynamics on Small UAVs. In Proceedings of the ION-GNSS Conference, Savannah, GA, USA, 16–19 September 2008.
5. Uhlig, D.; Sareen, A.; Sukumar, P.; Rao, A.H.; Selig, M.S. Determining Aerodynamic Characteristics of a Micro Air Vehicle Using Motion Tracking. In Proceedings of the AIAA Paper 2010-8416, AIAA Guidance, Navigation, and Control Conference, Toronto, ON, Canada, 2–5 August 2010. [CrossRef]
6. Dantsker, O.D.; Selig, M.S. High Angle of Attack Flight of a Subscale Aerobatic Aircraft. In Proceedings of the AIAA Paper 2015-2568, AIAA Applied Aerodynamics Conference, Dallas, TX, USA, 22–26 June 2015. [CrossRef]
7. Mockli, M. Guidance and Control for Aerobatic Maneuvers of an Unmanned Airplane. Ph.D. Thesis, ETH Zurich, Department of Mechanical and Process Engineering, Zurich, Switzerland, 2006.
8. Frank, A.; McGrewy, J.S.; Valentiz, M.; Levinex, D.; How, J.P. Hover, Transition, and Level Flight Control Design for a Single-Propeller Indoor Airplane. In Proceedings of the AIAA Paper 2007-6318, AIAA Guidance, Navigation, and Control Conference, Hilton Head, SC, USA, 20–23 August 2007. [CrossRef]
9. Johnson, E.N.; Wu, A.D.; Neidhoefer, J.C.; Kannan, S.K.; Turbe, M.A. Test Results of Autonomous Airplane Transitions Between Steady-Level and Hovering Flight. *J. Guid. Control Dyn.* **2008**, *31*, 358–370. [CrossRef]
10. Johnson, B.; Lind, R. Trajectory Planning for Sensing Effectiveness with High Angle-of-Attack Flight Capability. In Proceedings of the AIAA Paper 2012-0276, AIAA Aerospace Sciences Meeting, Nashville, TN, USA, 9–12 January 2012. [CrossRef]
11. Jordan, T.L.; Bailey, R.M. NASA Langley's AirSTAR Testbed: A Subscale Flight Test Capability for Flight Dynamics and Control System Experiments. In Proceedings of the AIAA Paper 2008-6660, AIAA Atmospheric Flight Mechanics Conference, Honolulu, HI, USA, 18–21 August 2008. [CrossRef]
12. Ragheb, A.M.; Dantsker, O.D.; Selig, M.S. Stall/Spin Flight Testing with a Subscale Aerobatic Aircraft. In Proceedings of the AIAA Paper 2013-2806, AIAA Applied Aerodynamics Conference, San Diego, CA, USA, 24–27 June 2013. [CrossRef]
13. Bunge, R.A.; Savino, F.M.; Kroo, I.M. Approaches to Automatic Stall/Spin Detection Based on Small-Scale UAV Flight Testing. In Proceedings of the AIAA Paper 2015-2235, AIAA Atmospheric Flight Mechanics Conference, Dallas, TX, USA, 22–26 June 2015. [CrossRef]
14. Dantsker, O.D.; Ananda, G.K.; Selig, M.S. GA-USTAR Phase 1: Development and Flight Testing of the Baseline Upset and Stall Research Aircraft. In Proceedings of the AIAA Paper 2017-4078, AIAA Applied Aerodynamics Conference, Denver, CO, USA, 5–9 June 2017. [CrossRef]
15. Risch, T.; Cosentino, G.; Regan, C.; Kisska, M.; Princen, N. X-48B Flight-Test Progress Overview. In Proceedings of the AIAA Paper 2009-934, AIAA Aerospace Sciences Meeting, Orlando, FL, USA, 5–8 January 2009. [CrossRef]
16. Lundstrom, D.; Amadori, K. Raven: A Subscale Radio Controlled Business Jet Demonstrator. In Proceedings of the International Congress on the Aeronautical Sciences Systems (ICUAS), Anchorage, AK, USA, 14–19 September 2008.
17. Regan, C.D.; Taylor, B.R. mAEWing1: Design, Build, Test—Invited. In Proceedings of the AIAA Paper 2016-1747, AIAA Atmospheric Flight Mechanics Conference, San Diego, CA, USA, 4–8 January 2016. [CrossRef]
18. Regan, C.D. mAEWing2: Conceptual Design and System Test. In Proceedings of the AIAA Paper 2017-1391, AIAA Atmospheric Flight Mechanics Conference, Grapevine, TX, USA, 9–13 January 2017. [CrossRef]
19. Leong, H.I.; Keshmiri, S.; Jager, R. Evaluation of a COTS Autopilot and Avionics System for UAVs. In Proceedings of the AIAA Paper 2009-1963, AIAA Infotech@Aerospace, Seattle, WA, USA, 6–9 April 2009. [CrossRef]
20. Esposito, J.F.; Keshmiri, S. Rapid Hardware Interfacing and Software Development for Embedded Devices Using Simulink. In Proceedings of the AIAA Paper 2010-3415, AIAA Infotech@Aerospace, Atlanta, GA, USA, 20–22 April 2010. [CrossRef]
21. Garcia, G.; Keshmiri, S. Integrated Kalman Filter for a Flight Control System with Redundant Measurements. In Proceedings of the AIAA Paper 2012-2499, AIAA Infotech@Aerospace, Garden Grove, CA, USA, 19–21 June 2012. [CrossRef]
22. Sobron, A.; Lundström, D.; Staack, I.; Krus, P. Design and Testing of a Low-Cost Flight Control and Data Acquisition System for Unstable Subscale Aircraft. In Proceedings of the International Congress on the Aeronautical Sciences Systems, Daejeon, Korea, 27–29 September 2016.
23. Theile, M.; Dantsker, O.D.; Caccamo, M.; Yu, S. uavAP: A Modular Autopilot Framework for UAVs. In Proceedings of the AIAA Paper 2020-3268, AIAA Aviation 2020 Forum, Virtual Event, 15–19 June 2020. [CrossRef]
24. Sukumar, P.P.; Selig, M.S. Dynamic Soaring of Sailplanes over Open Fields. *J. Aircr.* **2013**, *50*, 1420–1430. [CrossRef]
25. Woodbury, T.; Dunn, C.; Valasek, J. Autonomous Soaring Using Reinforcement Learningfor Trajectory Generation. In Proceedings of the AIAA Paper 2014-0990, AIAA SciTech Forum, National Harbor, Maryland, 13–17 January 2014. [CrossRef]
26. Depenbusch, N.T.; Bird, J.J.; Langelaan, J.W. The AutoSOAR autonomous soaring aircraft, part 1: Autonomy algorithms. *J. Field Robot.* **2016**. [CrossRef]

27. Sachs, G.; Gruter, B. Maximum TravelSpeed Performance of Albatrossesand UAVs Using Dynamic Soaring. In Proceedings of the AIAA Paper 2019-0568, AIAA SciTech Forum, San Diego, CA, USA, 7–11 January 2019. [CrossRef]

28. Bird, J.J.; Langelaan, J.W. Optimal Speed Scheduling for Hybrid Solar Aircraft with Arrival Time Condition. In Proceedings of the AIAA Paper 2019-1421, AIAA SciTech Forum, San Diego, CA, USA, 7–11 January 2019. [CrossRef]

29. Brandt, S.A.; Stiles, R.J.; Bertin, J.J.; Whitford, R. *Introduction to Aeronautics: A Design Perspective*, 3rd ed.; American Institute of Aeronautics and Astronautics, Inc.: Reston, VA, USA, 2015.

30. Howe, D. *Aircraft Conceptual Design Synthesis*; Professional Engineering Publishing Limited: Suffolk, UK, 2000.

31. Kundu, A.K. *Aircraft Design*; Cambridge University Press: Cambridge, UK, 2012.

32. McMasters, J.; Cummings, R. Rethinking the Airplane Design Process—An Early 21st Century Perspective. In Proceedings of the AIAA Paper 2004-693, AIAA Aerospace Sciences Meeting, Reno, NV, USA, 5–8 January 2004. [CrossRef]

33. Nicolai, L.M.; Carichner, G.E. *Fundamentals of Aircraft and Airship Design: Volume I— Aircraft Design*; American Institute of Aeronautics and Astronautics, Inc.: Reston, VA, USA, 1975.

34. Roskam, J. *Aircraft Design 1–8 Set*, 2nd ed.; Darcorporation: Lawrence, KS, USA, 2003.

35. Sadraey, M.H. *Aircraft Design: A Systems Engineering Approach*; John Wiley & Sons: West Sussex, UK, 2013.

36. Torenbeek, E. *Synthesis of Subsonic Airplane Design*; Delft University Press: Delft, The Netherlands, 1982.

37. Fielding, J.P. *Introduction to Aircraft Design*; Cambridge University Press: Cambridge, UK, 1999.

38. Keane, A.J.; Sóbester, A.; Scanlan, J.P. *Small Unmanned Fixed-Wing Aircraft Design: A Practical Approach*; John Wiley & Sons: West Sussex, UK, 2017.

39. Raymer, D.P. *Aircraft Design: A Conceptual Approach*, 5th ed.; American Institute of Aeronautics and Astronautics, Inc.: Reston, VA, USA, 2012.

40. Davenport, C. *Virgin Galactic's Quest for Space*; The Washington Post: Washington, DC, USA, 2018.

41. Stevenson, B. Virgin Galactic seeks 'year of rebirth'. *Flight Int.* **2015**, *187*, 10.

42. Raymer, D.P. Enhancing Aircraft Conceptual Design Using Multidisciplinary Optimization. Ph.D. Thesis, Swedish Royal Institute of Technology (KTH), Department of Aeronautics, Stockholm, Sweden, 2002.

43. Mainini, L.; Maggiore, P. Multidisciplinary Integrated Framework for the Optimal Design of a Jet Aircraft Wing. *Int. J. Aerosp. Eng.* **2012**, *2012*, 750642. [CrossRef]

44. Magnussen, O.; Hovland, G.; Ottestad, M. Multicopter UAV design optimization. In Proceedings of the IEEE International Conference on Mechatronic and Embedded Systems and Applications (MESA), Senigallia, Italy, 10–12 September 2014. [CrossRef]

45. Oktay, T.; Konar, M.; Onay, M.; Aydin, M.; Mohamed, M.A. Simultaneous small UAV and autopilot system design. *Aircr. Eng. Aerosp. Technol.* **2016**, *88*, 818–834. [CrossRef]

46. Fujiwara, G.E.C.; Bragg, M.B. Optimization of Variable-Camber Continuous Trailing-Edge Flap Configuration for Drag Reduction. *J. Aircr. Mar.* **2019**, *56*, 730–746. [CrossRef]

47. Maldonado, V.; Santos, D.; Wilt, M.; Ramirez, D.; Shoemaker, J.; Ayele, W.; Beeson, B.; Lisby, B.; Zamora, J.; Antu, C. 'Switchblade': Wide-Mission Performance Design of a Multi-Variant Unmanned Aerial System. In Proceedings of the AIAA Paper 2021-0213, AIAA SciTech Forum, Virtual Event, 11–15 January 2021. [CrossRef]

48. Kennedy, B.M.; Sobek, D.K.; Kennedy, M.N. Reducing rework by applying set-based practices early in the systems engineering process. *Syst. Eng.* **2013**, *17*, 278–296. [CrossRef]

49. Lundstrom, D.; Amadori, K.; Krus, P. Automation of Design and Prototyping of Micro Aerial Vehicle. In Proceedings of the AIAA Paper 2009-629, AIAA Aerospace Sciences Meeting, Orlando, FL, USA, 5–8 January 2009. [CrossRef]

50. Lundstrom, D. Aircraft Design Automation and Subscale Testing. Ph.D. Thesis, Linkoping University, Department of Management and Engineering, Linkoping, Sweden, 2012.

51. Dantsker, O.D.; Imtiaz, S.; Caccamo, M. Electric Propulsion System Optimization for a Long-Endurance Unmanned Aircraft. In Proceedings of the AIAA Paper 2019-4486, AIAA/IEEE Electric Aircraft Technologies Symposium, Indianapolis, IN, USA, 22–24 August 2019. [CrossRef]

52. Dantsker, O.D.; Theile, M.; Caccamo, M. A High-Fidelity, Low-Order Propulsion Power Model for Fixed-Wing Electric Unmanned Aircraft. In Proceedings of the AIAA Paper 2018-5009, AIAA/IEEE Electric Aircraft Technologies Symposium, Cincinnati, OH, USA, 9–11 July 2018. [CrossRef]

53. Laminar Research. X-Plane 11. Available online: http://www.x-plane.com/ (accessed on 31 January 2022).

54. InertiaSoft, Inc. FS One RC Flight Simulator. Available online: http://www.fsone.com/ (accessed on 31 January 2022).

55. Dantsker, O.D.; Yu, S.; Vahora, M.; Caccamo, M. Flight Testing Automation to Parameterize Unmanned Aircraft Dynamics. In Proceedings of the AIAA Paper 2019-3230, AIAA Aviation and Aeronautics Forum and Exposition, Dallas, TX, USA, 17–21 June 2019. [CrossRef]

56. Dantsker, O.D.; Deters, R.W.; Caccamo, M. Propulsion System Testing for a Long-Endurance Solar-Powered Unmanned Aircraft. In Proceedings of the AIAA Paper 2019-3688, AIAA Applied Aerodynamics Conference, Dallas, TX, USA, 17–21 June 2019. [CrossRef]

57. Dantsker, O.D.; Vahora, M.; Imtiaz, S.; Caccamo, M. High Fidelity Moment of Inertia Testing of Unmanned Aircraft. In Proceedings of the AIAA Paper 2018-4219, AIAA Applied Aerodynamics Conference, Atlanta, GA, USA, 25–29 June 2018. [CrossRef]

58. Mancuso, R.; Dantsker, O.D.; Caccamo, M.; Selig, M.S. A Low-Power Architecture for High Frequency Sensor Acquisition in Many-DOF UAVs. In Proceedings of the International Conference on Cyber-Physical Systems, Berlin, Germany, 14–17 April 2014. [CrossRef]

59. Dantsker, O.D.; Mancuso, R.; Selig, M.S.; Caccamo, M. High-Frequency Sensor Data Acquisition System (SDAC) for Flight Control and Aerodynamic Data Collection Research on Small to Mid-Sized UAVs. In Proceedings of the AIAA Paper 2014-2565, AIAA Applied Aerodynamics Conference, Atlanta, GA, USA, 16–20 June 2014. [CrossRef]

60. Dantsker, O.D.; Caccamo, M.; Vahora, M.; Mancuso, R. Flight & Ground Testing Data Set for an Unmanned Aircraft: Great Planes Avistar Elite. In Proceedings of the AIAA Paper 2020-0780, AIAA SciTech Forum, Orlando, FL, USA, 6–10 January 2020. [CrossRef]

61. Al Volo LLC. Al Volo: Flight Systems. Available online: http://www.alvolo.us (accessed on 31 January 2022).

62. Dantsker, O.D.; Mancuso, R. Flight Data Acquisition Platform Development, Integration, and Operation on Small- to Medium-Sized Unmanned Aircraft. In Proceedings of the AIAA Paper 2019-1262, AIAA SciTech Forum, San Diego, CA, USA, 7–11 January 2019. [CrossRef]

63. Canin, D.G.; McConnell, J.K.; James, P.W. F-35 High Angle of Attack Flight Control Development and Flight Test Results. In Proceedings of the AIAA Paper 2019-3227, AIAA Aviation and Aeronautics Forum and Exposition, Dallas, TX, USA, 17–21 June 2019. [CrossRef]

64. Qadri, M.; Vahora, M.; Hascaryo, R.; Finlon, S.; Dantsker, O.D.; Ananda, G.K.; Selig, M.S. Undergraduate Contribution to Dynamically Scaled General Aviation Research at the University of Illinois at Urbana-Champaign. In Proceedings of the AIAA Paper 2018-1069, AIAA Aerospace Sciences Meeting, Kissimmee, FL,USA, 8–12 January 2018. [CrossRef]

65. Kimberlin, R.D. *Flight Testing of Fixed-Wing Aircraft*; AIAA Education Series; AIAA: Reston, VA, USA, 2003.

66. McCormick, B.W. *Introduction to Flight Testing and Applied Aerodynamics*; AIAA Education Series; AIAA: Reston, VA, USA, 2011.

67. Ward, D.T.; Strganac, T.W. *Introduction to Flight Test Engineering*, 2nd ed.; Kendall/Hunt Publishing Company: Dubuque, IA, USA, 2001.

68. Arent, L.; Falatko, J. 757 fly-by-wire demonstrator flight test. In Proceedings of the AIAA Paper 1992-4099, 6th AIAA Biennial Flight Test Conference, Hilton Head, SC, USA, 24–26 August 1992. [CrossRef]

69. Brandon, J.M.; Morelli, E.A. Real-Time Onboard Global Nonlinear Aerodynamic Modeling from Flight Data. In Proceedings of the AIAA Paper 2014-2554, AIAA Atmospheric Flight Mechanics Conference, Atlanta, GA, USA, 16–20 June 2014. [CrossRef]

70. Larsson, R.; Sobron, A.; Lundström, D.; Enqvist, M. A Method for Improved Flight Testing of Remotely Piloted Aircraft Using Multisine Inputs. *Aerospace* **2020**, *7*, 135. [CrossRef]

71. Roessler, C.; Stahl, P.; Sendner, F.; Hermanutz, A.; Koeberle, S.; Bartasevicius, J.; Rozov, V.; Breitsamter, C.; Hornung, M.; Meddaikar, Y.M.; et al. Aircraft Design and Testing of FLEXOP Unmanned Flying Demonstrator to Test Load Alleviation and Flutter Suppression of High Aspect Ratio Flexible Wings. In Proceedings of the AIAA Paper 2019-1813, AIAA SciTech Forum, San Diego, CA, USA, 7–11 January 2019. [CrossRef]

72. Federal Aviation Administration, U.S. Department of Transportation. SUMMARY OF SMALL UNMANNED AIRCRAFT RULE (PART 107). Available online: https://www.faa.gov/uas/media/Part_107_Summary.pdf (accessed on 31 January 2022).

73. Dorobantu, A.; Johnson, W.; Lie, F.A.; Taylor, B.; Murch, A.; Paw, Y.C.; Gebre-Egziabher, D.; Balas, G. An airborne experimental test platform: From theory to flight. In Proceedings of the 2013 American Control Conference, Washington, DC, USA, 17–19 June 2013; pp. 659–673. [CrossRef]

74. Sobron, A.; Lundström, D.; Larsson, R.; Krus, P.; Jouannet, C. Methods For Efficient Flight Testing And Modelling Of Remotely Piloted Aircraft within Visual Line-of-Sight. In Proceedings of the International Congress on the Aeronautical Sciences Systems, Belo Horizonte, Brazil, 9–14 September 2018.

75. Stahl, P.; Sendner, F.M.; Hermanutz, A.; Rößler, C.; Hornung, M. Mission and Aircraft Design of FLEXOP Unmanned Flying Demonstrator to Test Flutter Suppression within Visual Line of Sight. In Proceedings of the AIAA Paper 2017-3766, AIAA Aviation Technology, Integration, and Operations Conference, Denver, CO, USA, 5–9 June 2017. [CrossRef]

76. Arifianto, O.; Farhood, M. Development and Modeling of a Low-Cost Unmanned Aerial Vehicle Research Platform. *J. Intell. Robot. Syst.* **2015**, *80*, 139–164. [CrossRef]

77. Sanders, F.C.; Tischler, M.; Berger, T.; Berrios, M.G.; Gong, A. System Identification and Multi-Objective Longitudinal Control Law Design for a Small Fixed-Wing UAV. In Proceedings of the AIAA Paper 2018-0296, AIAA Atmospheric Flight Mechanics Conference, Kissimmee, FL, USA, 8–12 January 2018. [CrossRef]

78. Murch, A. A Flight Control System Architecture for the NASA AirSTAR Flight Test Infrastructure. In Proceedings of the AIAA Paper 2008-6990, AIAA Guidance, Navigation and Control Conference, Honolulu, HI, USA, 18–21 August 2008. [CrossRef]

79. Napolitano, M.R. Development, Instrumentation, and Flight Testing of UAVs as Research Platforms for Flight Control Systems Research. Available online: http://www.dsea.unipi.it/Members/polliniw/sgn/sem_napolitano1 (accessed on 19 March 2013).

80. Reiss, P.; Dollinger, D.; Schropp, C.; Löbl, D.; Holzapfel, F. Multi Crew Coordination for Remote Piloted Transition VTOL. In Proceedings of the AIAA Paper 2021-1056, AIAA Scitech 2021 Forum, Virtual Forum, 11–21 January 2021. [CrossRef]

81. Sobron, A.; Lundström, D.; Krus, P. A Review of Current Research in Subscale Flight Testing and Analysis of Its Main Practical Challenges. *Aerospace* **2021**, *8*, 74. [CrossRef]

82. Factory, U. UAV Factory | Education. Available online: https://uavfactory.com/en/education (accessed on 31 January 2022).

83. Bunge, R.A.; Savino, F.M.; Kroo, I.M. Stall/Spin Flight Test Techniques with COTS Model Aircraft and Flight Data Systems. In Proceedings of the AIAA Paper 2015-3225, AIAA Flight Testing Conference, Dallas, TX, USA, 22–26 June 2015. [CrossRef]

84. Dantsker, O.D. Determining Aerodynamic Characteristics of an Unmanned Aerial Vehicle using a 3D Scanning Technique. In Proceedings of the AIAA Paper 2015-0026, AIAA Aerospace Sciences Meeting, Kissimmee, FL, USA, 5–9 January 2015. [CrossRef]

85. ZCorporation. The New ZScanner 800. Available online: www.zcorp.com/documents/182_ZScanner800-tearsheet-v05wb.pdf (accessed on 12 March 2013).

86. UIUC Applied Aerodynamics Group. UIUC Airfoil Coordinates Database. Available online: http://aerospace.illinois.edu/m-selig/ads/coord_database.html (accessed on 31 January 2022).

87. Dantsker, O.D.; Vahora, M. Comparison of Aerodynamic Characterization Methods for Design of Unmanned Aerial Vehicles. In Proceedings of the AIAA Paper 2018-0272, AIAA Aerospace Sciences Meeting, Kissimmee, FL, USA, 8–12 January 2018. [CrossRef]

88. Koeberle, S.J.; Albert, A.E.; Nagel, L.H.; Hornung, M. Flight Testing for Flight Dynamics Estimation of Medium-Sized UAVs. In Proceedings of the AIAA Paper 2021-1526, AIAA SciTech Forum, Virtual Event, 11–21 January 2021. [CrossRef]

89. Miller, M.P. An Accurate Method of Measuring the Moments of Inertia of Airplanes, 1930. National Advisory Committee for Aeronautics, Technical Note 351. Available online: https://ntrs.nasa.gov/citations/19930081105 (accessed on 31 January 2022).

90. Soule, H.; Miller, M.P. The Experimental Determination of the Moments of Inertia of Airplanes, 1934. National Advisory Committee for Aeronautics, Technical Note 467. Available online: https://ntrs.nasa.gov/citations/19930091541 (accessed on 31 January 2022).

91. Gracey, W. The Experimental Determination of the Moments of Inertia of Airplanes by a Simplified Compound -Pendulum Method, 1948. National Advisory Committee for Aeronautics, Technical Note 1629. Available online: https://ntrs.nasa.gov/citations/19930082299 (accessed on 31 January 2022).

92. Turner, H.L. Measurement of the Moments of Inertia of an Airplane by a Simplified Method, 1950. National Advisory Committee for Aeronautics, Technical Note 2201. Available online: https://ntrs.nasa.gov/citations/19930082849 (accessed on 31 January 2022).

93. de Jong, R.C.; Mulder, J.A. Accurate Estimation of Aircraft Inertia Characteristics from a Single Suspension Experiment. *J. Aircr.* **1987**, *24*, 362–370. [CrossRef]

94. Jardin, M.; Mueller, E. Optimized Measurements of UAV Mass Moment of Inertia with a Bifilar Pendulum. In Proceedings of the AIAA Paper 2007-6822, AIAA Guidance, Navigation, and Control Conference, Hilton Head, SC, USA, 20–23 August 2007. [CrossRef]

95. Bowman, A.; Barnes, G.; Keshmiri, S. An Empirical Method for Estimating Moments of Inertia of Light Unmanned Air Vehicles. In Proceedings of the AIAA Paper 2012-2598, AIAA Infotech@Aerospace, Garden Grove, CA, USA, 19–21 June 2012. [CrossRef]

96. Mendes, A.; van Kampen, E.; Remes, B.; Chu, Q. Determining moments of inertia of small UAVs: A comparative analysis of an experimental method versus theoretical approaches. In Proceedings of the AIAA Paper 2012-4463, AIAA Guidance, Navigation and Control Conference, Minneapolis, MN, USA, 13–16 August 2012. [CrossRef]

97. Lehmkühler, K.; Wong, K.; Verstraete, D. Methods for accurate measurements of small fixed wing UAV inertial properties. *Aeronaut. J.* **2016**, *120*, 1785–1811. [CrossRef]

98. McCormick, B.W. *Aerodynamics, Aeronautics, and Flight Mechanics*; Wiley: Hoboken, NJ, USA, 1994.

99. Pieper, K.; Perry, A.; Ansell, P.; Bretl, T. Design and Development of a Dynamically Scaled Distributed Electric Propulsion Aircraft Testbed. In Proceedings of the AIAA Paper 2018-4996, AIAA/IEEE Electric Aircraft Technologies Symposium, Cincinnati, OH, USA, 9–11 July 2018. [CrossRef]

100. Theile, M.; Dantsker, O.D.; Nai, R.; Caccamo, M. uavEE: A Modular, Power-Aware Emulation Environment for Rapid Prototyping and Testing of UAVs. In Proceedings of the IEEE International Conference on Embedded and Real-Time Computing Systems and Applications, Hakodate, Japan, 28–31 August 2018. [CrossRef]

101. National Science Foundation. Award Abstract 1932529: CPS: Medium: Collaborative Research: Virtual Sully: Autopilot with Multilevel Adaptation for Handling Large Uncertainties. Available online: https://www.nsf.gov/awardsearch/showAward?AWD_ID=1932529&HistoricalAwards=falsel (accessed on 31 January 2022).

102. Ponniah, J.; Yee, A.K.; Dantsker, O.D.; Yu, S.; Mancuso, R. Design of Multi-Agent UAV Simulator to Support the Development of the MARSNet Communication Protocol. In Proceedings of the AIAA Paper 2019-3114, AIAA Aviation and Aeronautics Forum and Exposition, Dallas, TX, USA, 17–21 June 2019. [CrossRef]

103. Lee, J.S.; Yu, K.H. Optimal Path Planning of Solar-Powered UAV Using Gravitational Potential Energy. *IEEE Trans. Aerosp. Electron. Syst.* **2017**, *53*, 1442–1451. [CrossRef]

104. Grano-Romero, C.; García-Juárez, M.; Guerrero-Castellanos, J.F.; Guerrero-Sánchez, W.F.; Ambrosio-Lázaro, R.C.; Mino-Aguilar, G. Modeling and control of a fixed-wing UAV powered by solar energy: An electric array reconfiguration approach. In Proceedings of the 2016 13th International Conference on Power Electronics (CIEP), Guanajuato, Mexico, 20–23 June 2016; pp. 52–57. [CrossRef]

105. Gao, X.Z.; Hou, Z.X.; Guo, Z.; Liu, J.X.; Chen, X.Q. Energy management strategy for solar-powered high-altitude long-endurance aircraft. *Energy Convers. Manag.* **2013**, *70*, 20–30. [CrossRef]

106. Hosseini, S.; Dai, R.; Mesbahi, M. Optimal path planning and power allocation for a long endurance solar-powered UAV. In Proceedings of the 2013 American Control Conference, Washington, DC, USA, 17–19 June 2013; pp. 2588–2593. [CrossRef]

107. B. Lee, B.; Park, P.; Kim, C.; Yang, S.; Ahn, S. Power managements of a hybrid electric propulsion system for UAVs. *J. Mech. Sci. Technol.* **2012**, *26*, 2291–2299. [CrossRef]

108. Ostler, J.; Bowman, W. Flight Testing of Small, Electric Powered Unmanned Aerial Vehicles. In Proceedings of the American Institute of Aeronautics and Astronautics, 2005, U.S. Air Force T&E Days Conferences, Nashville, TN, USA, 6–8 December 2005. [CrossRef]

109. Karabetsky, D. Solar rechargeable airplane: Power system optimization. In Proceedings of the 2016 4th International Conference on Methods and Systems of Navigation and Motion Control (MSNMC), Kiev, Ukraine 18–20 October 2016; pp. 218–220. [CrossRef]

110. Park, H.B.; Lee, J.S.; Yu, K.H. Flight evaluation of solar powered unmanned flying vehicle using ground testbed. In Proceedings of the 2015 15th International Conference on Control, Automation and Systems (ICCAS), Busan, Korea, 13–16 October 2015; pp. 871–874. [CrossRef]

111. Lindahl, P.; Moog, E.; Shaw, S.R. Simulation, Design, and Validation of an UAV SOFC Propulsion System. *IEEE Trans. Aerosp. Electron. Syst.* **2012**, *48*, 2582–2593. [CrossRef]

112. Bradt, J.B.; Selig, M.S. Propeller Performance Data at Low Reynolds Numbers. In Proceedings of the AIAA Paper 2011-1255 AIAA Aerospace Sciences Meeting, Orlando, FL, USA, 4–7 January 2011. [CrossRef]

113. Shiau, J.K.; Ma, D.M.; Chiu, C.W.; Shie, J.R. Optimal Sizing and Cruise Speed Determination for a Solar-Powered Airplane. *AIAA J. Aircr.* **2010**, *47*, 622–629. [CrossRef]

114. Ol, M.; Zeune, C.; Logan, M. Analytical/Experimental Comparison for Small Electric Unmanned Air Vehicle Propellers. In Proceedings of the 26th AIAA Applied Aerodynamics Conference; American Institute of Aeronautics and Astronautics: Reston, VA, USA, 18–21 August 2008. [CrossRef]

115. Brandt, J.; Deters, R.; Ananda, G.; Dantsker, O.; Selig, M. UIUC Propeller Database. Available online: http://m-selig.ae.illinois.edu/props/propDB.html (accessed on 31 January 2022).

116. Drela, M. First-Order DC Electric Motor Model. Available online: http://web.mit.edu/drela/Public/web/qprop/motor1_theory.pdf (accessed on 31 January 2022).

117. Drela, M. Second-Order DC Electric Motor Model. Available online: http://web.mit.edu/drela/Public/web/qprop/motor2_theory.pdf (accessed on 31 January 2022).

118. Gong, A.; MacNeill, R.; Verstraete, D. Performance Testing and Modeling of a Brushless DC Motor, Electronic Speed Controller and Propeller for a Small UAV. In Proceedings of the AIAA Paper 2018-4584, AIAA Propulsion and Energy Forum, Cincinnati, OH, USA, 9–11 July 2018. [CrossRef]

119. Green, C.R.; McDonald, R.A. Modeling and Test of the Efficiency of Electronic Speed Controllers for Brushless DC Motors. In Proceedings of the AIAA Paper 2015-3191, AIAA Aviation Forum, Dallas, TX, USA, 22–26 June 2015. [CrossRef]

120. McCrink, M.H.; Gregory, J.W. Blade Element Momentum Modeling for Low-Re Small UAS Electric Propulsion Systems. In Proceedings of the AIAA Paper 2015-3296, AIAA Aviation Forum, Dallas, TX, USA, 22–26 June 2015. [CrossRef]

121. Lundstrom, D.; Amadori, K.; Krus, P. Validation of Models for Small Scale Electric Propulsion Systems. In Proceedings of the AIAA Paper 2010-483, AIAA Aerospace Sciences Meeting, Orlando, FL, USA, 4–7 January 2010. [CrossRef]

122. McDonald, R.A. Modeling of Electric Motor Driven Propellers for Conceptual Aircraft Design. In Proceedings of the AIAA Paper 2015-1676, AIAA Aerospace Sciences Meeting, Kissimmee, FL, USA, 5–9 January 2015. [CrossRef]

123. Dantsker, O.D.; Selig, M.S.; Mancuso, R. A Rolling Rig for Propeller Performance Testing. In Proceedings of the AIAA Paper 2017-3745, AIAA Applied Aerodynamics Conference, Denver, CO, USA, 5–9 June 2017. [CrossRef]

124. Brandt, J.B. Small-Scale Propeller Performance at Low Speeds. Master's Thesis, University of Illinois at Urbana-Champaign, Department of Aerospace Engineering, Urbana, IL, USA, 2005.

125. Lundstrom, D.; Krus, P. Testing of Atmospheric Turbulence Effects on the Performance of Micro Air Vehicles. *Int. J. Micro Air Veh.* **2012**, *4*, 133–149. [CrossRef]

126. Uhlig, D.V. Post Stall Propeller Behavior at Low Reynolds Numbers. Master's Thesis, Department of Aerospace Engineering, University of Illinois at Urbana-Champaign, Urbana, IL, USA, 2007.

127. Uhlig, D.V.; Selig, M.S. Post Stall Propeller Behavior at Low Reynolds Numbers. In Proceedings of the AIAA Paper 2008-407, AIAA Aerospace Sciences Meeting, Reno, NV, USA, 7–10 January 2008. [CrossRef]

128. Deters, R.W.; Selig, M.S. Static Testing of Micro Propellers. In Proceedings of the AIAA Paper 2008-6246, AIAA Applied Aerodynamics Conference, Honolulu, HI, USA, 18–21 August 2008. [CrossRef]

129. Chaney, C.S.; Bahrami, J.K.; Gavin, P.A.; Shoemake, E.D.; Barrow, E.S.; Matveev, K.I. Car-Top Test Module as a Low-Cost Alternative to Wind Tunnel Testing of UAV Propulsion Systems. *J. Aerosp. Eng.* **2014**, *27*, 06014005. [CrossRef]

130. Deters, R.W. Performance and Slipstream Characteristics of Small-Scale Propelllers at Low Reynolds Numbers. Ph.D. Thesis, Department of Aerospace Engineering, University of Illinois at Urbana-Champaign, Urbana, IL, USA, 2014.

131. Deters, R.W.; Kleinke, S.; Selig, M.S. Static Testing of Propulsion Elements for Small Multirotor Unmanned Aerial Vehicles. In Proceedings of the AIAA Paper 2017-3743, AIAA Aviation Forum, Denver, CO, USA, 5–9 June 2017. [CrossRef]

132. Gong, A.; Verstraete, D. Experimental Testing of Electronic Speed Controllers for UAVs. In Proceedings of the AIAA Paper 2017-4955, AIAA/SAE/ASEE Joint Propulsion Conference, Atlanta, GA, USA, 10–12 July 2017. [CrossRef]

133. Gong, A.; Maunder, H.; Verstraete, D. Development of an in-fight thrust measurement system for UAVs. In Proceedings of the AIAA Paper 2017-5092, AIAA/SAE/ASEE Joint Propulsion Conference, Atlanta, GA, USA, 10–12 July 2017. [CrossRef]

134. Deters, R.W.; Dantsker, O.D.; Kleinke, S.; Norman, N.; Selig, M.S. Static Performance Results of Propellers Used on Nano, Micro, and Mini Quadrotors. In Proceedings of the AIAA Paper 2018-4122, AIAA Aviation Forum, Atlanta, GA, USA, 25–29 June 2018. [CrossRef]
135. Drela, M. DC Motor/Propeller Matching. Available online: http://web.mit.edu/drela/Public/web/qprop/motorprop.pdf (accessed on 31 January 2022).
136. Drela, M. QPROP. Available online: http://web.mit.edu/drela/Public/web/qprop/ (accessed on 31 January 2022).
137. McDonald, R.A. Modeling of Electric Motor Driven Variable Pitch Propellers for Conceptual Aircraft Design. In Proceedings of the AIAA Paper 2016-1025, AIAA Aerospace Sciences Meeting, San Diego, CA, USA, 4–8 January 2016. [CrossRef]
138. MacNeill, R.; Verstraete, D.; Gong, A. Optimisation of Propellers for UAV Powertrains. In Proceedings of the AIAA Paper 2017-5090, AIAA/SAE/ASEE Joint Propulsion Conference, Atlanta, GA, USA, 10–12 July 2017. [CrossRef]
139. MacNeill, R.; Verstraete, D. Optimal Propellers for a Small Hybrid Electric Fuel-Cell UAS. In Proceedings of the AIAA Paper 2018-4981, AIAA Propulsion and Energy Forum, Cincinnati, OH, USA, 9–11 July 2018. [CrossRef]
140. Landing Products Inc. APC Propellers. Available online: https://www.apcprop.com/ (accessed on 31 January 2022).
141. Noth, A. Design of Solar Powered Airplanes for Continuous Flight. Ph.D. Thesis, ETH Zurich, Zurich, Switzerland, 2008.
142. Oettershagen, P.; Melzer, A.; Mantel, T.; Rudin, K.; Stastny, T.; Wawrzacz, B.; Hinzmann, T.; Leutenegger, S.; Alexis, K.; Siegwart, R. Design of small hand-launched solar-powered UAVs: From concept study to a multi-day world endurance record flight. *J. Field Robot.* **2017**, *34*, 1352–1377. [CrossRef]
143. Real Time and Embedded System Laboratory, University of Illinois at Urbana-Champaign. Solar-Powered Long-Endurance UAV for Real-Time Onboard Data Processing. Available online: http://rtsl-edge.cs.illinois.edu/UAV/ (accessed on 31 January 2022).